Table of Contents

1. INTRODUCTION

The inverted pendulum is a benchmark problem for control courses, as it is analogues to many real-world control problems such as missile stabilization, Segway's, rockets and robotics etc [1]. The inverted pendulum is an unstable, nonlinear, under- actuated and Single Input-Multiple Output (SIMO) system [1]. This makes the design and implementation of a controller challenging. Consequently, the inverted pendulum problem has constantly been a research interest for control engineers [1].

The purpose of this report is to present the modelling and simulation of both single and double linked pendulum systems with one degree of dimensional freedom (i.e. movement along the x-axis). Additionally, a microphone based measurement subsystem is employed. A control system is thus, implemented to stabilize the system i.e. maintain the desired vertical position. The performance of the controllers on the system should be analysed and relative performance is critiqued and evaluated.

The structure of the report is as follows: Section 2 is the background concerning the problem. Section 3 is modelling with regards to both single and double pendulums using both Lagrangian and Newtonian methods. Section 4 is modelling with regards to the microphone measurement system. Section 5 describes, implements the different controllers utilized. Section 6 is the results of the controllers for both single and double pendulum implementation. Section 7 critically analyses the solution. Section 8 proposes future recommendations and Section 9 is presents conclusions.

2. BACKGROUND

2.1. Requirements

The primary requirements are as follows:

- Modelling and simulation of a single linked inverted pendulum system in one direction of freedom.
- Lagrangian Modelling must be used
- Modelling and simulation of microphone based measurement subsystem.
- Development and Simulation of a single control system to stabilize the inverted pendulum.

The secondary requirements are as follows:

- Modelling and simulation of a multi linked inverted pendulum system in one direction of freedom (e.g. double linked inverted pendulum).
- Modelling and simulation of multiple measurement subsystems.
- Development, Simulation and comparison of a multiple different controllers used to stabilize the inverted pendulum.

2.2. Constraints

The constraints for the project are as follows:

- A period of approximately a month to complete the task.
- MATLAB and Simulink can only be used.

2.3. Assumptions

The assumptions are as follows:

- There is access to all the pendulum states, except the one that is to be measured by the microphone.
- The system is a rigid body.
- There is no relative sliding.
- The transfer delay between the subsystems is negligible.
- Frictionless system.
- The pendulum is starting in an upright position (equilibrium of 0 rad).

2.4. Success criteria

The success criteria for the project is defined as follows: The successful modelling and simulation of a double linked, single degree of motion inverted pendulum with corresponding microphone based measurement system. Additionally, two controllers will be implemented with the goal of having transient behaviour with 10% overshoot and 2 seconds settling time.

2.5. Literature review

As mentioned previously, stabilization of an inverted pendulum is of great research interest as it has numerous applications in various sectors including aeronautics and robotics. The Inverted Pendulum is a SIMO system hence making control challenging. From the relevant literature, it can be observed that the modelling of the inverted pendulum can be done either using the Lagrangian equations or by Newtonian Force Analysis [2,3]. The Lagrangian method derives the system equations by applying the Euler-Lagrange equation [3]. The difference between kinetic and potential energy is how the Lagrangian is defined [3]. The system is then linearized around the desired equilibrium point using Taylor series and using small angle approximations. This will limit operation to within a small deviation from the vertical position. The Jacobian Linearization produces matrices necessary for the state space format [4]. It has also been seen that as the number of links

increase, correspondingly there is an increase in the complexity of the equations of the pendulum system[5]. There are numerous existing methodologies of control for an inverted pendulum. In a paper by Jose et al.[7], the author compares both the use of LQR and PD controllers applied to a double inverted pendulum. Both types of controllers successfully control the linearized double inverted pendulum. The angles and distance is successfully controlled. The LQR controller outperforms the PD in terms of performance characteristics of both the carts position and both the pendulum angles.

Khashayar et al [8] proposes Fuzzy logic control for an inverted pendulum. A brief review of Fuzzy Logic was given with its relation to a conventional controller. This information is then used to derive a Fuzzy Logic controller specifically for an inverted pendulum. The performance of the Fuzzy Logic controller was compared to conventional PID or state feedback controllers. The Fuzzy Logic controller providing better results by being more robust. The conventional controller performance heavily depends on the parameters of the system. Khashayar et al. [8] recommends the use of Fuzzy Logic, for very complex systems where there is no mathematical model.

A comparison between LQR, double-PID and pole placement controller on a single pendulum was conducted by Shehu [9]. The performances of the proposed controllers were investigated based on response time specifications and level of disturbance rejection; with the LQR preforming the best. To summarize the research of controllers, the best preforming controller for a specific pendulum depends on the parameter of the system. Thus, controller choice is based on suitability to the parameters.

Existing literature with regard to measurement systems indicate that typically the angle of the pendulum and can be measured by using either using tilt sensor, gyro sensor or potentiometer [10]. There are typically no sensors on the cart itself. An estimator is then used to get the other necessary states [11].

2.6. Particular Solution

Considering the relevant literature, the particular solution will consist of:
(1) Single and double inverted pendulum system.
(2) A capacitor based microphone subsystem, which will have an input of velocity (to calculate force) and measuring cart displacement.
(3) Controllers: state feedback using pole placement, LQR, PID and Fuzzy Logic control.
(4) A Luenberger Full state observer to estimate the other states from the output of the microphone.
(5) Desired transient behaviour of 2 second settling time and 10% overshoot.

A system overview can be seen in Figure 1.

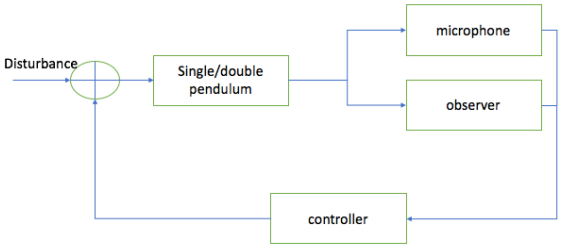

Figure 1: High systems overview of complete system with controller

3. PENDULUM ON A CART MODELLING

Modelling will be done using both Lagrangian and Newtonian Force Analysis.

3.1. Single Linked Inverted Pendulum

Table 1 contains the parameters utilized for the single inverted pendulum
.

Table 1: Single Inverted Pendulum parameters

Parameter	Specifications
Mass of cart	1 kg
Mass of pendulum	0.2 kg
Length of pendulum	0.3 m
Damping factor of cart	0.1 N s/m
Gravitational force	9.81

Figure 2 below shows a single inverted pendulum on a cart, which will be used to derive the equations using the force and Lagrangian analysis.

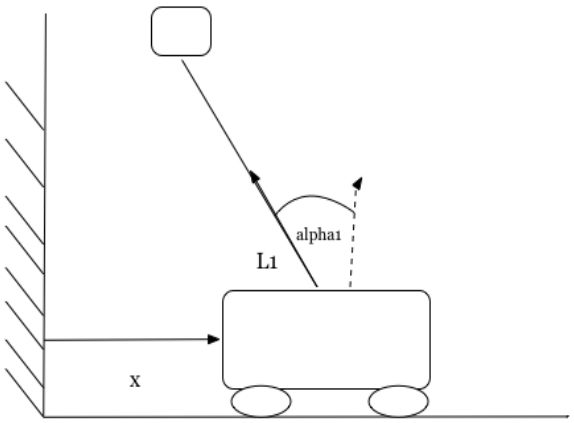

Figure 2: Diagram of single inverted pendulum.

3.1.1. Force Analysis

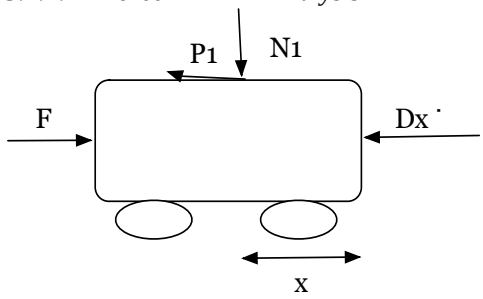

Figure 3: Forces on cart of single pendulum.

Taking the force in the x-direction of Figure 3 and using Newton's Second Law, Equation 1 is derived

$$\ddot{x} = {}^{1}/_{M}\,[F - p1 - D\dot{x}] \quad (1)$$

Where:
M is the mass of the cart.
P1 is the normal force of the pendulum in the x direction
F is the force applied
$D\dot{x}$ is the resistive force

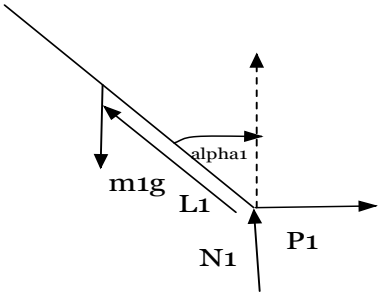

Figure 4: Forces on pendulum

Taking the force in the x-direction and y direction of Figure 4 and using Newton's Second Law, Equation 2 and 3 is derived

$$m\frac{d^2}{dt^2}(x + Lsin\theta) = p1 \quad (2)$$

$$m\frac{d^2}{dt^2}(Lcos\theta) = n1 \quad (3)$$

Where:
m is mass of pendulum
θ is the angle of the pendulum
x is the horizontal distance
n1 is is the normal force of the pendulum in the y direction

Taking Newton's Second Law for rotation around the centre of gravity

$$I\frac{d}{dt^2}^{2}\,\theta = n1Lsin\theta - p1(Lcos\theta) \quad (4)$$

$$I = {}^{1}/_{3}\,ml^2 \quad (5)$$

where: I
eliminating the reaction force gives the 2 equations below

$$(M+m)\ddot{x} + b\dot{x} - mlsin\theta\dot{\theta}^2 + mlcos\theta\ddot{\theta} = u \quad (6)$$

$$m\ddot{x}cos\theta + mlsin\ddot{\theta} = mgsin(\theta) \quad (7)$$

3.1.2. Lagrange Analysis

The Lagrangian equation is defined as

$$L = ke - p \quad (8)$$

where:
L is the Lagrangian equation
ke is the kinetic energy of the system
p is the potential energy of the system

The x position of the pendulum is defined as x+lsinθ and the y position is lcosθ where θ is the angle of the pendulum.

$$ke = {}^{1}/_{2}\,M\dot{x}^2 + {}^{1}/_{2}\,m\left(\frac{d}{dt}(x + lsin\theta)\right)^2 + {}^{1}/_{2}\,m\left(\frac{d}{dt}(lcos\theta)\right)^2 \quad (9)$$

$$p = mgl(1 - cos\theta) \quad (10)$$

The Lagrangian is defined in Equation 11

$$L = {}^{1}/_{2}\,(M+m)\dot{x}^2 + ml\dot{x}cos\theta + {}^{1}/_{2}\,ml^2\dot{\theta}^2 - mgl(1 - cos\theta) \quad (11)$$

Taking the partial derivative as define by Equation 12 below produces Equations 13 and 14 below taking friction force into account.

$${}^{d}/_{dt}\left({}^{\partial l}/_{\partial \dot{x}_i}\right) - {}^{\partial l}/_{dx_i} + {}^{\partial P}/_{\partial \dot{x}_i} = U_i \quad (12)$$

$$(M+m)\ddot{x} + b\dot{x} - mlsin\theta\dot{\theta}^2 + mlcos\theta\ddot{\theta} = u \quad (13)$$

$$m\ddot{x}cos\theta + mlsin\ddot{\theta} = mgsin(\theta) \quad (14)$$

3.1.3. Linearization of model

A linear model is then derived from equation 13 and 14 by taking the Jacobian and using small angle approximations where sin $\theta = \theta$ and cos $\theta = 1$.

$$(M+m)\ddot{x} + b\dot{x} - ml\theta\dot{\theta}^2 + ml\ddot{\theta} = u \quad (15)$$

$$m\ddot{x} + ml\ddot{\theta} = mg\theta \quad (16)$$

$$\frac{d}{dt}\,\Delta\,\dot{x} = -{}^{b}/_{m}\,\Delta\,\dot{x} + {}^{m}/_{M}\left(l\dot{\theta}^2 - g\right)\Delta\,\theta + {}^{2ml\theta\dot{\theta}}/_{M}\,\Delta\,\dot{\theta} + {}^{1}/_{m}\,\Delta\,u \quad (17)$$

$$\frac{d}{dt}\,\Delta\,\dot{\theta} = {}^{b}/_{lm}\,\Delta\,\dot{x} + ({}^{g(M+m)}/_{lm} - {}^{m\dot{\theta}^2}/_{M})\,\Delta\,\theta - {}^{2ml\theta\dot{\theta}}/_{M}\,\Delta\,\dot{\theta} - {}^{1}/_{m}\,\Delta\,u \quad (18)$$

The state space using equation 17 and 18 is as

$$\frac{d}{dt}\begin{pmatrix}\Delta\theta\\ \Delta\dot{\theta}\\ \Delta x\\ \Delta\dot{x}\end{pmatrix} = \begin{pmatrix}0 & 1 & 0 & 0\\ g(M+m)/lM & 0 & 0 & b/lm\\ 0 & 0 & 0 & 1\\ -mg/M & 0 & 0 & -b/m\end{pmatrix}\begin{pmatrix}\Delta\theta\\ \Delta\dot{\theta}\\ \Delta x\\ \Delta\dot{x}\end{pmatrix} + \begin{pmatrix}0\\ -1/m\\ 0\\ 1/m\end{pmatrix}\Delta u$$

3.1.4. Simulink Implementation

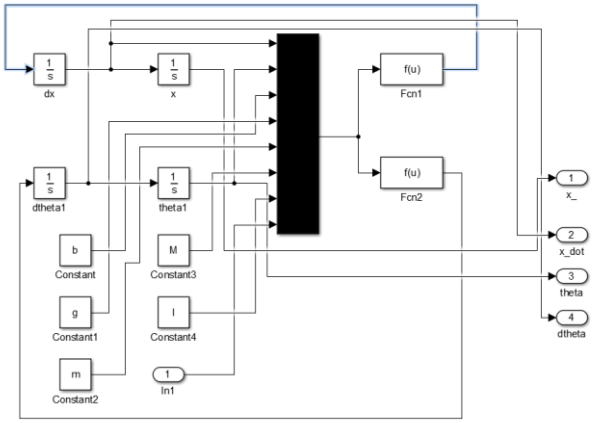

Figure 5: Simulink implementation of single pendulum microphone.

Figure 5 above shows the Simulink implementation of the linearized single pendulum model which used the mux constants and functions.

- **Open Loop Behaviour**

After modelling of the system, as well as, linearization the open loop behaviour of the system (i.e. with no controller) should be characterised.

The linearized system is expressed in the form of equation. Using MATLAB the transfer function of the linearized system is derived and the closed-loop poles are obtained. A system is only stable if all the closed loop poles lie in the left half of the 's' plane. The following poles in the Root Locus in Figure 6 are obtained for the system. Clearly, the system is unstable as there are poles in the right hand plane.

Not only are there poles in the right hand plane, but also the right-most pole converges toward positive infinity and hence, further confirming the system instability.
Lastly, the inherent instability of the system was confirmed on Simulink. Using initial conditions (initially displacing the pendulum) for θ_1 of 0.1 rad. It can be seen in Figures that the angle of the pendulum exponentially increases toward infinity. This relationship is indicative of an unstable system.

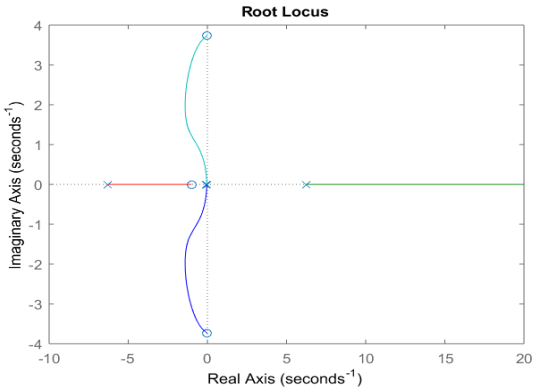

Figure 6: Root Locus of the single linked pendulum

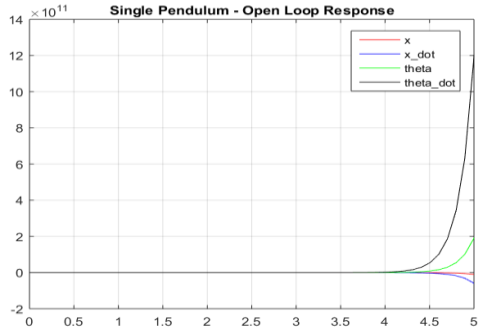

Figure 7: Open Loop behaviour of single linked pendulum

3.2. Double Linked Inverted Pendulum

Both Force and Lagrange analysis is done for the system.

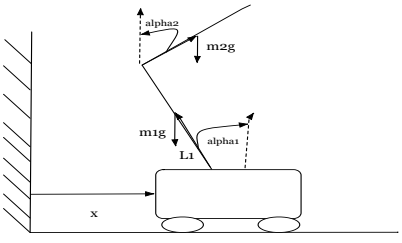

Figure 8: Diagram of double inverted pendulum.

Table 2 contains the parameters used for the double inverted pendulum.

Table 2: Double Inverted Pendulum parameters

Parameter	Specifications
Mass of cart	1 kg
Mass of first pendulum	0.5 kg
Mass of second pendulum	0.25 kg
Length of first pendulum	0.25 m
Length of second pendulum	0.25 m
Gravitational force	9.81m/s^2

3.2.1. Force Analysis

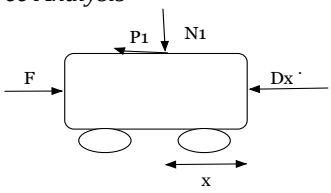

Figure 9: Forces on cart of double pendulum.

The forces on the cart can be seen in equation 19 below

$$\ddot{x} = {}^{1}/_{M}\,[f - n1 - D\dot{x}] \quad (19)$$

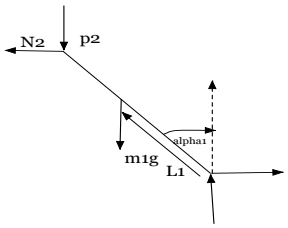

Figure 10: Free body diagram of first pendulum

Horizontal distance to centre of mass of first pendulum can be seen in equation 20

$$x1 = x - l1sin\theta1 \quad (20)$$

where:
x1 is the total horizontal distance of the first pendulum
x is the distance of the cart
l1 is the length to the centre of mass of that pendulum
$\theta1$ is the angle of the first pendulum

$$\dot{x}1 = \dot{x} - \dot{\theta}1l1cos\theta1 \quad (21)$$

$$\ddot{x1} = \ddot{x} + \dot{\theta}1^2 l1sin\theta1 - 1l1cos\,\theta1 \quad (22)$$

$$y1 = l1cos\theta1 \quad (23)$$

where:
y1 is the total vertical distance of the first pendulum
Using Newtons Second Law on forces and rotations

$$m1\ddot{x} + n2 = n1 \quad (24)$$

$$m1\ddot{y} = P1 - m1 \quad (25)$$

$$P1 = m1\ddot{y} + m1 \quad (26)$$

$$\ddot{\theta}1 = {}^{1}/_{I1}\,[N1l1cos\theta1 + P1l1sin\theta1 + b1\dot{\theta}1 + N2l1cos\theta1 + P2l1sin\theta1] \quad (27)$$

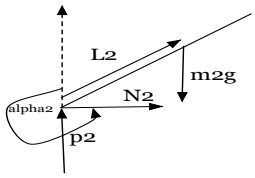

Figure 11: Free body diagram of second pendulum

Horizontal distance to centre of mass of first pendulum can be seen in Equation 28

$$x2 = x - 2l1sin\theta1 - l2sin\theta2 \quad (28)$$

where:
x2 is the total distance of the second pendulum
l2 is the length to the centre of mass for the second pendulum
$\theta2$ is the angle of the second pendulum

$$\dot{x}1 = \dot{x} - \dot{\theta}1l1cos\theta1 \quad (29)$$

$$\ddot{x1} = \ddot{x} + \dot{\theta}1^2 l1sin\theta1 - \ddot{\theta}1l1cos\,\theta1 \quad (30)$$

$$y1 = l1cos\theta1 \quad (31)$$

where:
y1 is the total vertical distance of the first pendulum

$$\dot{y1} = -\dot{\theta}1^2 l1sin\theta1 \quad (32)$$

$$\ddot{y1} = -\dot{\theta}1^2 l1cos\theta1 + \ddot{\theta}1l1sin\,\theta \quad (33)$$

$$m1\ddot{x} = n1 - n2 \quad (34)$$

where:
m1 is the mass of the pendulum

$$\dot{x}2 = \dot{x} - 2\dot{\theta}1l1cos\theta1 - \dot{\theta}2l2cos\theta2(1)\ddot{x}2 = \ddot{x} + 2\dot{\theta}1^2 l1sin\theta1 - 2\ddot{\theta}1l1cos\,\theta1 + \dot{\theta}2^2 l2sin\theta2 - \ddot{\theta}2l2cos\,\theta \quad (35)$$

$$y2 = 2l1cos\theta1 + l2cos\theta2 \quad (36)$$

$$\dot{y}2 = -2\dot{\theta}1^2 l1sin\theta1 - \dot{\theta}2l2sin\theta2 \quad (37)$$

$$\ddot{y}2 = -2\dot{\theta}1^2 l1cos\theta1 + 2\ddot{\theta}1l1sin\,\theta1 - \dot{\theta}2^2 l2cos\theta2 - \ddot{\theta}2l2sin\,\theta2 \quad (38)$$

$$m2\ddot{x} = n2 \quad (39)$$

$$m2\ddot{y} = P2 - m2g \quad (40)$$

$$P2 = m2\ddot{y} + m2g \quad (41)$$

$$\ddot{\theta}2 = {}^{1}/_{I2}\left[N2l2cos\theta2 + P2l2sin\theta2 - b2\dot{\theta}2\right] \quad (42)$$

3.2.2. Lagrange Analysis

$$k\ (cart) = {}^{1}/_{2}\,mv^2 \quad (43)$$

$$k1 = {}^{1}/_{2}\,m1[(\dot{x}^2 - \dot{\theta}1l1cos\theta1)^2 + (l1cos\theta1)^2] + {}^{1}/_{2}\,I1\dot{\theta}1^2 \quad (43)$$

$$= {}^{1}/_{2}\,m1\dot{x}^2 + {}^{1}/_{2}\,(m1l1^2 + I1)\dot{\theta}1^2 + m1l1\dot{x}1\dot{\theta}1\ cos\theta1 \quad (44)$$

where:
k1 is the kinetic energy of the first pendulum

$$k2 = {}^{1}/_{2}\,m1\dot{x}^2 + {}^{1}/_{2}\,m2l1^2\dot{\theta}1^2 + {}^{1}/_{2}\,(m2l2^2 + I2)\dot{\theta}2^2 + m2l1\dot{x}1\dot{\theta}1\ cos\theta1 + m2l2\dot{x}1\dot{\theta}2\ cos\theta2 + m2l2l1\dot{\theta}1\ \dot{\theta}2\cos(\theta1 - \theta2) \quad (45)$$

where:
k2 is the kinetic energy of the second pendulum.

$$Po = 0 \quad (46)$$

where:
P0 is the potential energy of the cart

$$p1 = m1gl1\ cos\theta1 \quad (47)$$

where:
P1 is the potential energy of the first pendulum

$$p2 = m2g(l1\ cos\theta1 + l2\ cos\theta1) \quad (48)$$

where:
P2 is the potential energy of the second pendulum

Solve using Lagrangian equation:

$$\begin{aligned} L &= k - p \\ &= {}^{1}/_{2}\,(m0 + m1 + m2)^2\dot{x}^2 \\ &+ {}^{1}/_{2}\,(m1l1^2 + m2l2^2 + I1)\dot{\theta}1^2 \\ &+ {}^{1}/_{2}\,(m2l2^2 + I2)\dot{\theta}2^2 \\ &+ (m1l1 + m2l1)cos\theta1\dot{x}^2\dot{\theta}1 + m2l2\cos\theta2\dot{\theta}2\dot{x} \\ &+ m2l1l2\cos(\theta1 - \theta2)\,\dot{\theta}1\dot{\theta}2 \\ &- (m1l1 + m2l1)gcos\theta1 \\ &- m2l2gcos\theta1 \end{aligned} \quad (49)$$

Partial derivatives are as follows:

$$d/_{dt}\left(\partial l/_{\partial\dot{x}}\right) - \partial l/_{dx} = F \quad (50)$$

$$d/_{dt}\left(\partial l/_{\partial\dot{\theta}1}\right) - \partial l/_{d\theta1} = 0 \quad (51)$$

$$d/_{dt}\left(\partial l/_{\partial\dot{\theta}2}\right) - \partial l/_{d\theta2} = 0 \quad (52)$$

$$F = (m0 + m1 + m2) + (m1l1 + m2l1)\ cos\theta1\ddot{\theta}1 + m2l2cos\theta2\ddot{\theta}2 - (m1l1 + m2l1)\ sin\theta1\dot{\theta}1^2 - m2l2sin\theta2\dot{\theta}2^2 \quad (53)$$

$$0 = (m1l1 + m2l1)\ cos\theta1\ddot{x} + (m1l1^2 + m2l1^2 + I1)\ddot{\theta}1 + m2l1l2\cos(\theta1 - \theta2)\,\ddot{\theta}2 + m2l1l2\cos(\theta1 - \theta2)\,\dot{\theta}2^2 - (m1l1 + m2l1)gcos\theta1 \quad (54)$$

$$0 = m2l2gcos\theta1\ddot{x} + m2l1l2\cos(\theta1 - \theta2)\,\ddot{\theta}1 + (m2l2^2 + I1)\ddot{\theta}2 - m2l1l2\sin(\theta1 - \theta2)\,\dot{\theta}2^2 - (m2l2)gsin\theta2 \quad (55)$$

Solving for $\ddot{\theta}1$ and $\ddot{\theta}2$ in equation 53, 54 and 55 gives equation 56 and 57.

$$\ddot{\theta}1 = {}^{1}/_{I1}\left[N1l1cos\theta1 + P1l1sin\theta1 + b1\dot{\theta}1 + N2l1cos\theta1 + P2l1sin\theta1\right] \quad (56)$$

$$\ddot{\theta}2 = {}^{1}/_{I2}\left[N2l2cos\theta2 + P2l2sin\theta2 - b2\dot{\theta}2\right] \quad (57)$$

3.2.3. Linearization of model

The Lagrange Model is linearised around 0 using equation 58 as well as using Jacobian partial derivatives and small angle approximations

$$D(\theta)\ddot{\theta} + C(\theta,\dot{\theta})\dot{\theta} + G(\theta) = Hu \quad (58)$$

$$l = L/2 \quad (59)$$

$$I = {}^{ml^2}/_{12} \quad (60)$$

$$D(\theta) = \begin{pmatrix} m0 + m1 + m2 & ({}^{m1}/_{2} + m2)l1cos\theta1 & {}^{m2l2}/_{2}\,cos\theta2 \\ ({}^{m1}/_{2} + m2)l1cos\theta1 & ({}^{m1}/_{3} + m2)l1^2 & {}^{m2l1l2}/_{2}\cos(\theta1 - \theta2) \\ {}^{m2l2}/_{2}\,cos\theta2 & {}^{m2l1l2}/_{2}\cos(\theta1 - \theta2) & {}^{m2l2^2}/_{3} \end{pmatrix} \begin{pmatrix} \ddot{x} \\ \ddot{\theta}1 \\ \ddot{\theta}2 \end{pmatrix}$$

$$C(\theta,\dot{\theta}) = \begin{pmatrix} 0 & ({}^{m1}/_{2} + m2)l1cos\theta1 & -{}^{m2l2}/_{2}\,sin\theta2\dot{\theta}2 \\ 0 & 0 & -{}^{m2l1l2}/_{2}\sin(\theta1 - \theta2)\dot{\theta}2 \\ 0 & -{}^{m2l1l2}/_{2}\sin(\theta1 - \theta2)\dot{\theta}1 & 0 \end{pmatrix} \begin{pmatrix} \dot{x} \\ \dot{\theta}1 \\ \dot{\theta}2 \end{pmatrix}$$

$$G(\theta) = \begin{pmatrix} 0 \\ -({}^{1}/_{2}\,m1 + m2) \\ -({}^{1}/_{2})m2l2gsin\theta2 \end{pmatrix} \begin{matrix} l1gsin\theta1 \end{matrix} \begin{pmatrix} x \\ \theta1 \\ \theta2 \end{pmatrix}$$

$$H = \begin{pmatrix} 1 \\ 0 \\ 0 \end{pmatrix} F$$

$$\dot{x} = Ax + Bu$$
$$y = Cx + Du$$

where:
x is the internal state
u is the inputs to the system
y is the measured output
A is matrix of the plant
B is matrix of control inputs
C is matrix of measurements
D is matrix of direct feed

$$Linearization\ point: (x, \theta1, \theta2, \dot{x}, \dot{\theta1}, \dot{\theta2}) = [0]$$

$$x = \begin{pmatrix} x \\ \theta1 \\ \theta2 \\ \dot{x} \\ \dot{\theta1} \\ \dot{\theta2} \end{pmatrix}$$

$$C(q)\ddot{q} + D(q, \dot{q})\dot{q} + G(q) = Gu$$

$$\ddot{q} = c^{-1}(Gu - D\dot{q} - E)$$

$$\dot{x} = \begin{bmatrix} \dot{q} \\ c^{-1}(Gu - D\dot{q} - E) \end{bmatrix} = f(x, u)$$

E=G($\theta1$)

$$= \begin{pmatrix} 0 \\ -(1/2\, m1 + m2) \\ -(1/2) m2 l2 g sin\theta2 \end{pmatrix} \quad l1 g sin\theta1 = \begin{pmatrix} 0 \\ -e1 sin\theta1 \\ -e2 sin\theta2 \end{pmatrix} \begin{pmatrix} x \\ \theta1 \\ \theta2 \end{pmatrix}$$

3.2.4. Simulink Implementation

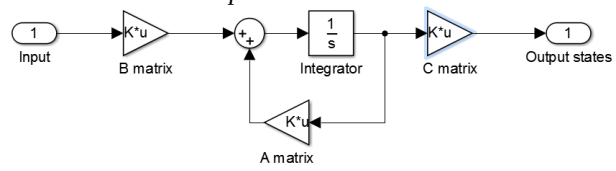

Figure 12: Simulink implementation of linearize double pendulum microphone.

Figure 12 above shows the Simulink implementation of the linearized double pendulum model which uses the state space function which makes implementation easier due to the high number of terms.

- Open Loop Behaviour

The open loop behaviour of the double pendulum system has the similar characteristics as the single pendulum system in terms of open loop behaviour, with poles in the RHP.

Much like the single pendulum system, this is confirmed on the double pendulum system with the root locus and plots of the system variables indicating instability of the open loop system. The Root Locus can be seen in Figure 13 with unstable poles in the RHP. Moreover, the open-loop behaviour is clearly shown as unstable in Figure 14 for a small angle deviation.

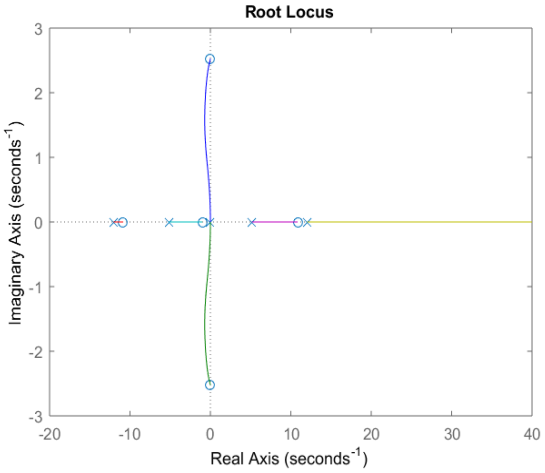

Figure 13: Root Locus of double inverted pendulum system

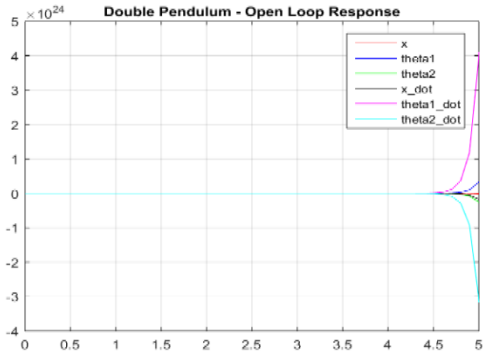

Figure 14: Open loop response of the double inverted pendulum system

4. MICROPHONE MEASUREMENT MODELLING

4.1. Theory of Measurement

N.B. Both Force and Lagrange analysis will be conducted.

The capacitive microphone utilized effectively operates as a force sensor (i.e. force on the capacitor plates). The force in this case is the force of drag (i.e. the force of the air on the plates). The drag force has a velocity term and this is assumed as the velocity of the cart.

The output measurement after calculations will be the carts displacement. This is possible due to there being some relationship between the plates of the capacitor which will either increase or decrease in size depending if the force of drag is applied onto the microphone or not. The force on the plate will cause the plates of the microphone to move. Thus, there will be a displacement

of the plates. From analysis (see Figure), the relationship between the displacement of the cart and that of the microphone plates is approximately linear.

The microphone plate displacement will thus be scaled/multiplied by some linear gain (of approximately 200) to match the carts displacement. The capacitive model of the microphone used can be seen in Figure 15 below:

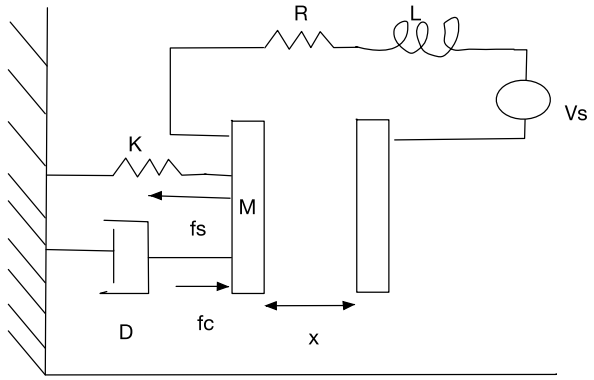

Figure 15: Simplified model of a capacitive microphone

Table 3 contains the parameters used for the microphone

Parameter	**Specifications**
Spring constant	1 N/m
Mass of microphone	0.5 kg
Damper constant	200 N s/m
Resistance	100 Ω
Inductance	0.0001 l
Epsilon	1 $F \cdot m^{-1}$
Area of plates	0.1 m^2

4.2. Force analysis

The microphone has both mechanical and electrical sub-systems which must be modelled.

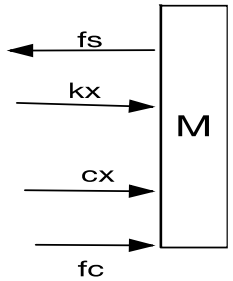

Figure 16: Free body diagram of Mechanical subsystem of microphone

$$Fres = ma$$
(61)
where:
fres is the resultant force
m is the mass of the moving object
a is the acceleration

$$fs - Kx - c\dot{x} - fc = m\ddot{x} \quad (62)$$
where:
fs is the drag force cause by the air on the plate
kx is the spring force of the spring on the plate
cx is the damper force of the spring on the plate
fc is the force of the capacitor on the plate.
M is the mass of the plate
x is the distance between the two capacitor plates

$$x1 = x \quad (63)$$
$$x2 = \dot{x}1 \quad (64)$$
where:
x2 is the velocity of the plates.

$$fs - Kx1 - cx2 - fc = m\dot{x}2 \quad (65)$$

$$\dot{x}2 = {}^{fs}/_{m} - {}^{kx1}/_{m} - {}^{Dx2}/_{m} - {}^{fc}/_{m} \quad (66)$$

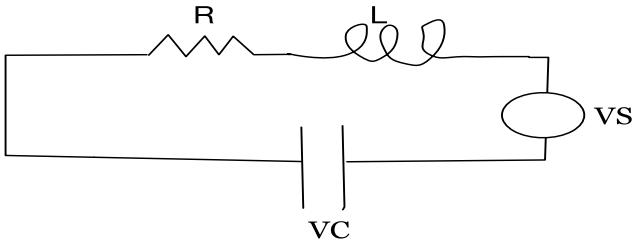

Figure 17: Electrical subsystem of microphone

Vloop=0 (67)
where:
vloop is the voltages in the circuit loop

$$+Vs - Vc - Vl - Vr = 0 \quad (68)$$
where:
Vs is the supply voltage.
Vc is the capacitor voltage
Vl is the inductor voltage
Vr is the resistor voltage

$$Vc = {}^{q}/_{c} \quad (69)$$
where:
q is the charge
c is the capacitance of the capacitor

$$Vl = L\ddot{q} \quad (70)$$

where:
L is the inductance of the inductor

$$Vr = R\dot{q} \quad (71)$$

where:
R is the resistance of the resistor

$$+Vs - {}^{q}/_{c} - L\ddot{q} - R\dot{q} = 0 \quad (72)$$

$$x3 = q \quad (73)$$

$$x4 = \dot{x}3 \quad (74)$$

where:
x4 is the current

$$+Vs - {}^{x3}/_{c} - L\dot{x}4 - Rx4 = 0 \quad (75)$$

$$\dot{x}4 = {}^{Vs}/_{l} - {}^{x3}/_{cl} - {}^{Rx4}/_{l} \quad (76)$$

4.3. Lagrange Analysis

$$ke = {}^{1}/_{2}\, m\dot{x}^2 + \frac{1}{2} l\dot{q}^2 \quad (77)$$

$$v = {}^{1}/_{2c}\, q^2 + {}^{1}/_{2}\, Kx^2 \quad (78)$$

$$c = {}^{\varepsilon A}/_{x_0 - x} \quad (79)$$

Where:
ε is epsilon
A is the area of the plates
Xo is the original position of the plates
X is the distance the plate have move

$$v = {}^{1}/_{2\varepsilon A}\, (x_0 - x)q^2 + {}^{1}/_{2}\, Kx^2 \quad (80)$$

$$l = {}^{1}/_{2}\, m\dot{x}^2 + \tfrac{1}{2} l\dot{q}^2 - {}^{1}/_{2\varepsilon A}\, (x_0 - x)q^2 - {}^{1}/_{2}\, Kx^2 \quad (81)$$

$$\partial l/_{\partial \dot{x}} = m\dot{x} \quad (82)$$

$$\partial l/_{\partial x} = {}^{q^2}/_{2\varepsilon A} - kx \quad (83)$$

$$\partial p/_{\partial \dot{x}} = B\dot{x} \quad (84)$$

Where:
B is the damping factor

$$dl/_{d\dot{q}} = l\dot{q} \quad (85)$$

$$dl/_{dq} = {}^{(x_0 - x)q}/_{\varepsilon A} \quad (86)$$

$$dp/_{d\dot{q}} = R\dot{q} \quad (87)$$

$$m\ddot{x} + Kx + D\dot{x} - {}^{q^2}/_{2\varepsilon A} = fs \quad (88)$$

$$+ {}^{(x_0 - x)q}/_{\varepsilon A} - L\ddot{q} - R\dot{q} = +Vs \quad (89)$$

4.4. Linearization of the model

$$x1 = x \quad (90)$$

$$x2 = \dot{x}1 \quad (91)$$

x3=q (92)

$$x4 = \dot{x}3 \quad (93)$$

$$\dot{x}2 = {}^{fs}/_{m} - K/_{m}\, x1 - D/_{m}\, x2 + {}^{x3^2}/_{2\varepsilon Am} \quad (94)$$

$$\dot{x}4 = {}^{Vs}/_{l} - {}^{(x_0 - x)q}/_{\varepsilon Al}\, x3 - {}^{R}/_{L}\, x4 \quad (95)$$

Solve for initial conditions

$$x2 = \dot{x}1 = 0 \quad (96)$$

$$x4 = \dot{x}1 = 0 \quad (97)$$

$$0 = fs - {}^{k}/_{m}\, x1 - Dx2 + {}^{x3^2}/_{22\varepsilon A} \quad (98)$$

$$x1 = {}^{f}/_{k} + {}^{1}/_{2\varepsilon Ak} \quad (99)$$

$$0 = Vs - {}^{(x_0 - x)}/_{\varepsilon A}\, x3 \quad (100)$$

sub 55 into 56

$$0 = vs - {}^{(x_0 - x)}/_{\varepsilon A}\, x3 + \left({}^{f}/_{k} + {}^{1}/_{2\varepsilon Ak}\, x3^2\right) x3 \quad (101)$$

Solving for the equilibrium points in equation 57 and 55 using the initial conditions gives the following equilibrium points.

$$x3 = \sqrt{2\varepsilon Akx_0} \quad (102)$$

$$x1 = x_0 \quad (103)$$

Taking the partial derivative with respect to x1,x2, x3 and x4 at the equilibrium points gives the following state space:

$$\begin{bmatrix} \dot{x}1 \\ \dot{x}2 \\ \dot{x}3 \\ \dot{x}4 \end{bmatrix} = \begin{pmatrix} 0 & 1 & 0 & 0 \\ -k/_{m} & -b/_{m} & \sqrt{2\varepsilon Akx_0}/_{\varepsilon Am} & 0 \\ 0 & 0 & 0 & 1 \\ 0 & 0 & 0 & -R/_{L} \end{pmatrix} \begin{pmatrix} x1 \\ x2 \\ x3 \\ x4 \end{pmatrix} + \begin{pmatrix} 0 \\ 0 \\ 0 \\ 1/_{l} \end{pmatrix} V + \begin{pmatrix} 0 \\ 1/_{m} \\ 0 \\ 0 \end{pmatrix} F$$

4.5. Simulink Implementation

The Simulink model of the linearised microphone is shown in Figure 18.

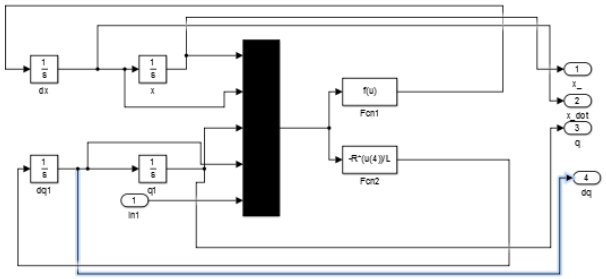

Figure 18: Simulink model of microphone

5. CONTROLLERS

Controllers are designed for both the linearized systems of the single and double inverted pendulums. Various types of controllers are explored such that the different controller topologies may be compared. Fundamentally, state feedback control will be explored, however optimal control (using LQR), intelligent control (using Fuzzy Logic) and classical control (using PID) will be used as comparisons.

For control of the single inverted pendulum the following controllers are explored: (1) State feedback (using pole placement), (2) LQR and (3) PID.

For control of the double inverted pendulum the following controllers are explored: (1) State feedback (using pole placement), (2) LQR, (3) Fuzzy Logic and (4) PID. Additionally, for the double inverted pendulum: a Luenberger Full state observer/estimator will be implemented linked to the controllers for situations where all states are not accessible and must be estimated prior to control of the system.

5.1. Single Linked Inverted Pendulum

5.1.1. Controllability and Observability

Before a controller can be designed the controllability and observability of the system must be determined as the outcomes of the tests significantly influence potential controller design. At worst case suggesting the system is uncontrollable (that a controller would have no impact).

The necessary and sufficient condition for controllability
From Burns [12] is: rank[$\mathbf{B : AB : } \boldsymbol{A^2}\mathbf{B}\boldsymbol{\ldots\ldots A^{n-1}}\mathbf{B}$]= n
Where: the dimension of matrix **A** is nxn.

In MATLAB the controllability matrix was manually generated using matrix algebra. The result was confirmed by making use of the *ctrb()* function built into MATLAB. The rank of the Controllability matrix is 6 which matches the n of matrix **A**. The implication is that the system is fully controllable with no uncontrollable states.
From MATLAB calculations the controllability matrix is as follows :

```
single_ctrb_matrix =

         0   -3.3333    0.3333 -130.8333
   -3.3333    0.3333 -130.8333   15.2633
         0    1.0000   -0.1000    6.5500
    1.0000   -0.1000    6.5500   -1.3090
```

The second test that must be carried out is Observability analysis of the systems states. The necessary and sufficient condition from Burns [12] is:
rank[$\boldsymbol{C^T : C^T A^T : C^T (A^T)^2 \ldots\ldots C^T (A^T)^{n-1}}$=n
Where: the dimension of matrix A is nxn.

In MATLAB the observability matrix was manually generated using matrix algebra, moreover the result was confirmed by making use of the *obsv()* function built into MATLAB. The rank of the Observability matrix is 6 which matches the size of matrix **A**. The implication is that the system states are fully observable.
From MATLAB calculations the observability matrix is as follows:

```
single_obs_matrix =

   1.0e+03 *

    0.0010    0.0010    0.0010    0.0010
    0.0373    0.0010         0    0.0012
    0.0368    0.0373         0    0.0002
    1.4624    0.0368         0    0.0124
```

Thus, the single pendulum system is fully controllable and observable.

5.1.2. State Feedback (Pole placement)

- *Theory of controller (State feedback control)*

A linear system state representation is given by the following 2 equations

$$\dot{\boldsymbol{x}} = \boldsymbol{Ax} + \boldsymbol{Bu} \quad (104)$$

$$\boldsymbol{y} = \boldsymbol{Cx} + \boldsymbol{Du} \quad (105)$$

where:
x is the internal state
u is the inputs to the system
y is the measured output
A is matrix of the plant
B is matrix of control inputs
C is matrix of measurements
D is matrix of direct feed

A control law [12] in the form of Equation 106 can be applied to the system

$$u = -\boldsymbol{K}x + r \quad (106)$$

where:
r is vector of desirable states
K is the state feedback matrix

Subbing the control law into the state space gives us Equation 107 below

$$\dot{x} = (A - bK)x + r \quad (107)$$

where
$(A - bK)$ is the close loop system matrix

The characteristic equation for the closed loop system [12] is defined in Equation 108 below

$$|sI - A + Bk| = 0 \quad (108)$$

Solving for the roots gives us the closed loop poles.

A control loop using state feedback can be seen in the Figure 19 below from [12].

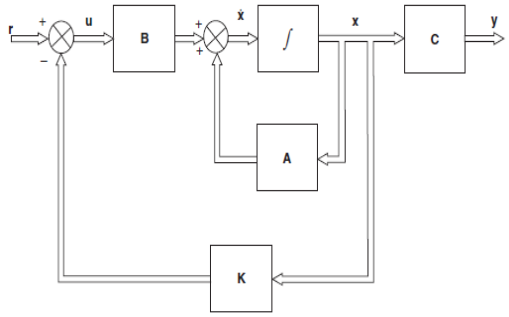

Figure 19: Control using state feedback (from [12])

The desired pole placement presents the problem of determining a **K** matrix with r equals to zero. This can be achieved in one of three ways according to Burns [12]. (1) Direct comparison method where the desired poles are chosen and solving Equation 109 below.

$$|sI - A + Bk| = (s1 - \mu_1) \ldots . (sn - \mu_n) \quad (109)$$

where:
μ_n is the value of the desired pole of nth pole.

(2) The Controllable Canonical Form where the K value is calculated directly using Equation 110 below.

$$k = [\alpha_0 - a_{0:}\ \alpha_1 - a_{1:} \ldots \ldots . . : \alpha_{n-1} - a_{n-1:}]T^{-1} \quad (110)$$

where:
T=MW
M is the controllable n by n matrix form
M= **[B:AB:……$A^{n-1}B$]**

W is the in the matrix show below

$$w = \begin{bmatrix} a_1 & a_2 & \cdots & a_{n-1} & 1 \\ a_2 & a_3 & \cdots & 1 & 0 \\ \vdots & 1 & \cdots & 0 & 0 \\ 1 & 0 & \cdots & 0 & 0 \end{bmatrix}$$

(3) Ackerman's formula defined by Equation 111 below

$$K = [0 \quad 0 \quad 0 \quad 0 \quad 1]M^{-1}\phi^{-1} \quad (111)$$

From the methods above the desired feedback matrix can be obtained. $u = -Kx$, The control will drive the system to zero from initial conditions of zero.

- *Controller Implementation*

Based on the theory discussed above, it is important to first define the desired closed loops poles. Thereby, define the desired closed loop characteristic equation.

Given that the system is **4th order** : two methods of pole placement will be explored in order to determine which method produces superior performance.

(1) Repeated poles: Define the dominant closed loop poles for desired performance for a 2nd order system and then repeat the set of poles at the same location in order to have 4 poles. (i.e. the dominant poles are repeated).

(2) Non-repeated poles: Define the dominant closed loop poles for specific performance. Then push the remaining 2 poles further left to reduce their influence. In this implementation, the poles are pushed 5 times further into the LHP.

The engineer often defines the system performance parameters, thus the desired transient behaviour for this scenario as:

Overshoot: 10%
Rise Time : 2 seconds

In a second order system, Equation 112 defines the generalized equation [12]:

$$s^2 + 2\zeta\omega_n + {\omega_n}^2 \quad (112)$$

Transient behaviour relates through Equations 113 and 114:

$$\text{Rise Time} = \frac{4}{\zeta\omega} \quad (113)$$

$$\%\ \text{Overshoot} = e^{-\frac{\zeta\pi}{\sqrt{1-\zeta^2}}} \quad (114)$$

Using the required transient behaviour and solving the above equations.

$$\zeta = 0.59115$$
$$\omega_n = 3.383$$

Solving Equation 112 using ζ & ω_n gives the following desired poles.

(1) Repeated Poles

μ1 = -1.999 + 2.728i
μ 2= -1.999 - 2.728i
μ3 = -1.999 + 2.728i
μ 4= -1.999 - 2.728i

(2) Non- repeated Poles

μ1 = -1.999 + 2.728i
μ 2= -1.999 - 2.728i
μ 3 = -9.999 + 13.643i
μ 4= -9.999 - 13.643i

The desired closed loop equation calculated using the above poles. The state feedback gain matrix (**K**) is then solved based on the Direct Comparison method shown in Equation 115.
The matrix manipulation is done manually in a MATLAB script and the result confirmed for accuracy using the *acker()* function which implements Ackerman's Formula of pole placement.

$$|s\boldsymbol{I} - \boldsymbol{A} + \boldsymbol{BK}| = (desired\ C.L\ equation)$$
(115)

The following state feedback gain matrices are obtained

(1) Repeated poles

K= [-24.64, -3.24, -4.00, -2.89]

(2) Non-repeated poles

K= [-155.08, -19.79, -100.14, -42.09]

- *Simulink implementation*

The Simulink model is illustrated in Figure. The gain block circled in red can be changed for different values of K.

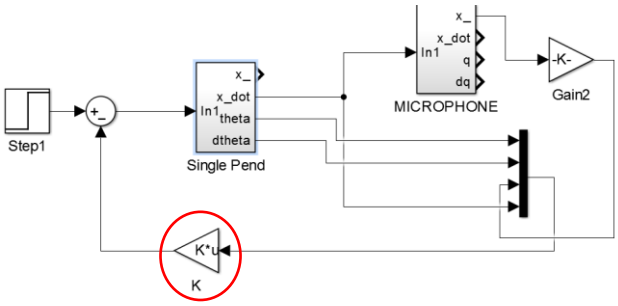

Figure 20: Simulink model of Single Pendulum with state feedback

5.1.3. Linear Quadratic Regulator (LQR)

- *Theory of controller (optimal control)*

The method of state feedback using pole placement is able to determine the **K** value for the state feedback matrix.

However, as a comparison a 2nd control approach of optimal control is explored. A Linear Quadratic Regulator (LQR) is used in the field optimal control. LQR aims to minimize the cost of controlling the system (i.e. control a system optimally).

Much like pole placement, LQR aims to find a **K** matrix to be applied to the linear control law of u= -**K**x. However, the aim of LQR is to minimize the cost function J defined by Equation 116 [12].

$$J=\int_{to}^{t1}(\boldsymbol{x}^T\boldsymbol{Q}\boldsymbol{x} + \boldsymbol{u}^T\boldsymbol{R}\boldsymbol{u})dt$$
(116)

Where: **x** is the state matrix
Q is a state weighting matrix
R is a control weighting matrix
u is the input matrix
J is the cost function (scalar)

The cost function (J) is a performance metric or indicator of the control process [12]. Effectively, the cost function can be thought of as the energy involved in the control process. The principle of LQR is that the state (x) and control input (u) are both weighted in J. The aim is to minimize J such that x and u are minimized as well. Thus, if x goes to 0 as time increases, it implies system stabilization.

The LQR model must be applied on a linear plant/system, whilst the cost function by its very nature is quadratic [12]. Once these two criteria are met, the Algebraic Riccati in Equation 117 can be solved for **P** [12]. The **Q** and **R** parameters are matrices that is set by the engineer/designer.

The Q matrix is a "penalty/weight matrix" [14]. The larger the value in the matrix associated with the respective state variable, the more we penalize the system if stabilization to is not achieved. The R matrix refers to the cost of control. However, the details of these matrices and the relationship to the model of the Q and R matrix will be discussed in the Critical analysis section.

$$\boldsymbol{PA} + \boldsymbol{A^T P} + \boldsymbol{Q} - \boldsymbol{PBR^{-1}B^T P} = 0 \quad (117)$$

Once P is determined from the Riccati Equation (Equation 117), the optimal LQR gain (**K**) can be solved as per Equation 118:

$$\boldsymbol{K}_{optimal} = \boldsymbol{R^{-1}B^T P} \quad (118)$$

- *Controller Implementation*

MATLAB was used to solve the Algebraic Riccati equation, as it is computationally expensive as a calculation. Thereafter, $\boldsymbol{K}_{optimal}$ was solved manually using matrix algebra calculations. The final answer of the optimal state gain matrix was confirmed by checking the calculation against the MATLAB function *lqr()*.

LQR requires the designer/engineer to define the weightings of the Q and R matrix. The aim is to ascertain the relationship of Q and R to performance.

Hence, 4 different combinations of Q and R are tested in order to see the impact of the weightings on transient behaviour.

The 4 combinations are: (1) Big Q, small R ; (2) Small Q, small R ;(3) Big Q, large R;; (4) small Q, large R.
(1) Big Q, Small R:

The following **Q** and **R** matrices, gives the following

$$\boldsymbol{Q} = diag(500, 0\ , 5000, 0)$$
R=1

$\boldsymbol{K}_{optimal}$ (1) = [-111.33,-18.72, -70.71,-37.98]

(2) Small Q, small R:

The following **Q** and **R** matrices, gives the following

$$\boldsymbol{Q} = diag(5000, 0\ , 100, 0)$$
R=1

$\boldsymbol{K}_{optimal}$ (2)= [-98.86, -11.58, -10.00, -13.43]

(3) Big Q, Large R:

The following **Q** and **R** matrices, gives the following

$$\boldsymbol{Q} = diag(500, 0\ , 5000, 0)$$
R=2

$\boldsymbol{K}_{optimal}$ (3) = [-90.49,-15.23,-49.99, -28.43]

(4) Small Q, Large R:

The following **Q** and **R** matrices, gives the following

$$\boldsymbol{Q} = diag(5000, 0, 100, 0)$$
R=2

$\boldsymbol{K}_{optimal}$ (4) = [-76.01, -9.54, -7.07, -9.72]

- *Simulink implementation*

The Simulink Model is the same as 5.1.2 (State Feedback using Pole placement). The only difference is that the feedback matrix K circled in red in Figure 20 would change to the K matrices calculated above.

5.1.4. PID Control

The implementation of a PID controller on the system could not be achieved.

The reason being that if one where to observe the Root Locus, in the Figure 6 , there is a pole in the RHP that tends to positive infinity for all values of k making it impractical and unfeasible to implement a PID.

A PID would be possible if we change the parameters of the system.

5.2. Double Linked Inverted Pendulum

5.2.1. Controllability and Observability

The proofs of controllability and observability follow the same theory as outlined for a single pendulum in Section 5.1.1.

The controllability matrix is:

```
double_ctrb_matrix =

   1.0e+04 *

         0    0.0001         0    0.0029         0    0.3756
         0   -0.0005         0   -0.0599         0   -8.4319
         0    0.0001         0    0.0391         0    6.3480
    0.0001         0    0.0029         0    0.3756         0
   -0.0005         0   -0.0599         0   -8.4319         0
    0.0001         0    0.0391         0    6.3480         0
```

The rank of the controllability matrix is: 6

The observability matrix is:

```
double_obs_matrix =

   1.0e+05 *

    0.0000    0.0000    0.0000    0.0000    0.0000    0.0000
         0    0.0004    0.0002    0.0000    0.0000    0.0000
         0    0.0004    0.0002         0    0.0004    0.0002
         0    0.0348   -0.0040         0    0.0004    0.0002
         0    0.0348   -0.0040         0    0.0348   -0.0040
         0    4.3796   -1.4468         0    0.0348   -0.0040
```

The rank of the observability matrix is: 6

A is a 6 x 6 matrix. Hence, from the theory outlined in section 5.1.1. It can be said the double inverted pendulum system is both fully observable and controllable

5.2.2. State Feedback (Pole placement)

- *Theory of controller (State feedback control)*
  Refer to Section 5.1.2.

- *Controller Implementation*

It was seen from the simulation of a single pendulum that performance of non-repeated poles was indeed superior (see Section 7.2). Thus, for the double inverted pendulum only non-repeated pole placement will be utilized.

Using the same transient parameters as in Section 5.1.2. The dominant poles are found to be the same as in Section 5.1.2.

The double inverted pendulum is a **6th order system** and hence, the chosen pole placements further left in the LHP are chosen as 3 times to the left and 5 times to the left of the dominant poles. Hence, the desired closed loop poles are:

μ1 = -1.999 + 2.728i
μ2= -1.999 - 2.728i
μ 3=-5.999 + 8.185i
μ 4=5.999- 8.185i
μ 5 = -9.999 + 13.643i
μ 6= -9.999 - 13.643i

The poles give the state feedback gain matrix **(K)**

K= [152.115 , -85.908, 410.585,
81.514, 19.739, 61.470]

- *Simulink*

The Simulink Model is illustrated in Figure 21.

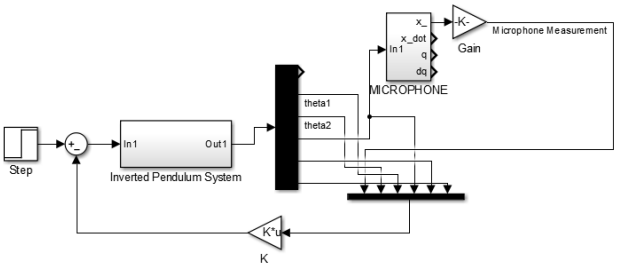

Figure 21: Simulink model of Double Pendulum with state feedback

5.2.3. Linear Quadratic Regulator (LQR)

- *Theory of controller (optimal control)*
  Refer to section 5.1.3.

- *Controller Implementation*

Similar to a single pendulum, a MATLAB script is run to solve the Algebraic Riccati Equation and moreover, matrix manipulations to solve for $\mathbf{K}_{\text{optimal}}$. The *lqr()* function was used to verify the answer.

Two different Q matrices are defined. The difference is: (1) Penalizes heavily for x $(cart\ displacement)$, θ_1 , θ_2 (2) Penalizes heavily for $\dot{x}$ $\dot{\theta}_1$ $\dot{\theta}_2$ not being zero

(1) Penalizes heavily for x $(cart\ displacement)$, θ_1 , θ_2

The following **Q** and **R** matrix, gives the following

$$\boldsymbol{Q} = diag(5000, 5000\ , 5000, 0,0,0)$$

R=1

$\boldsymbol{K}_{optimal}$ (1) = [70.71,-158.57, 443.68,
66.01, 15.66, 69.66]

(2) Penalizes heavily for $\dot{x}$ $\dot{\theta}_1$ $\dot{\theta}_2$ not being zero

$$\boldsymbol{Q} = diag(5, 50\ , 50, 20, 700, 700)$$

R=1

$\boldsymbol{K}_{optimal}$ (2) = [2.23, -403.74, 483.05,
7.99, -14.12, 75.15]

- *Simulink Implementation*

The Simulink Model is the same as 5.2.2 (State Feedback using Pole placement). The only difference is that the feedback matrix K circled in red in Figure 21, would change to the K matrix calculated above.

5.2.4. Fuzzy Logic Control (Intelligent control)

- *Theory of controller*

The controllers methodologies discussed previously: state feedback using pole placement or LQR and PID all require a mathematical model of the system in order to design a controller [8,12]. However, in cases such as the double inverted pendulum, the model is both non-linear and complicated. Thus, any model approximates the system model with some tolerance.

A Fuzzy Logic controller does not experience these problems, as it does not require knowledge of the systems mathematical model [8,12]. In fact, Fuzzy Logic controllers simply can be designed through heuristic/ experimental data [12]. Since, inverted pendulums have long been investigated there is a plethora of heuristic data about pendulum behaviour.

It can thus, be said that a Fuzzy Logic controller is a knowledge-based controller [12] and design is simply based on known system behaviour.

In designing a Fuzzy Logic controller, rules must be defined about the system. The rules are based on IF – THEN logic. However, a problem arises that Kumar et al [13] terms "rule explosion". In a double inverted pendulum system with 6 states (n) and an input, will have 7 membership functions (m). This would require m^n rules, which in this case is 117649 rules.

The sheer magnitude of the number of rules required is problematic, especially in terms of computation time.
A solution to reduce the number of rules, yet still have adequate performance is proposed by both Wang et al [14] and Kumar et al [13].

The proposal is a Fuzzy Logic Controller using a LQR based Information Fusion Function [13,14].

In the state feedback loop, the fusion function synthesizes $x\ (cart\ displacement)$, θ_1 , θ_2 into a single error variable and $\dot{x}$, $\dot{\theta}_1$ and $\dot{\theta}_2$ into a single rate of change of error variable [13,14].

Thus, rather than all 6 states feeding into the Fuzzy Logic Controller, only 2 variables feed into the controller: (1) Error and (2) Rate of change of error.

The rational behind this decision is that there is a significant coupling of variables in an inverted pendulum system – hence the errors may be amalgamated.

The information fusion function is certainly computationally beneficial as it reduces the number of required rules to $7^2 = 49$ rules instead of 117649 rules.

According to Wang et al [14] and Kumar et al [13], the Information Fusion Function can be generated using LQR methods (see Section 5.2.3). The optimal feedback gain matrix from LQR , is **K** = [k1, k2, k3 , k4, k5 , k6].

The co-efficients in the **K** matrix is used to synthesise the Fusion Function (F).

$$F=\begin{bmatrix} \frac{k1}{k3} & \frac{k2}{k3} & 1 & 0 & 0 & 0 \\ 0 & 0 & 0 & \frac{k4}{k6} & \frac{k5}{k6} & 1 \end{bmatrix}$$

The output of the Fusion Function is:

$$\begin{bmatrix} Error \\ \Delta Error \end{bmatrix} = F(x)\ x^T$$

The Error and $\Delta Error$ are fed into the Fuzzy Logic Controller as per Figure.

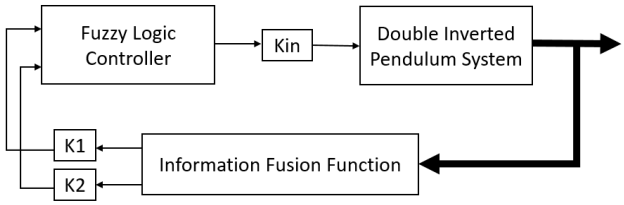

Figure 22: System with Fuzzy Logic and Fusion Function based on [13] and [14]

In terms of the actual Fuzzy Logic controller, typically there are 7 states: Positive Big (PB), Positive Medium (PM), Positive Small (PS), Zero (Z), Negative Small (NS), Negative Medium (NM) and Negative Big (NB) and typically triangular shapes are used to define these 7 states of Error and $\Delta Error$.

An easy rule table defines the rules related to the input states. Table 4 defines the rules utilized and is based on those used by [13] and [14].

The rules in Table 4 are added to the Fuzzy Logic controller based on IF-THEN relationships. With the output of the controller being the outcome the relation.

In terms of the process of output defuzzification. It is proposed that single input systems use the Mamdani type inference, whereas multi-input system should use Sugeno type inference. The theory of the inference processes are not within the scope of this paper, however, the decision is relevant for Simulink Application. The double pendulum system is SIMO, thus Mamdani is used.

Table 4: Fuzzy Logic Rule Table

	NB	NM	NS	Z	PS	PM	PB	$\Delta Error$
NB	NB	NB	NB	NM	NM	NS	Z	
NM	NB	NB	NM	NM	NS	Z	PS	
NS	NB	NM	NM	NS	Z	PS	PM	
Z	NM	NM	NS	Z	PS	PM	PM	
PS	NM	NS	Z	PS	PM	PM	PB	
PM	NS	Z	PS	PM	PM	PB	PB	
PB	Z	PS	PM	PM	PB	PB	PB	
Error								

- *Controller Implementation*

The Fuzzy Logic Toolbox in MATLAB is used to implement the Fuzzy Logic controller. The rule base in Table 4 is defined within the toolbox shown in Figure 23.

The example of the implemented input set is shown in Figure 24, whilst the output set is illustrated in Figure 25.

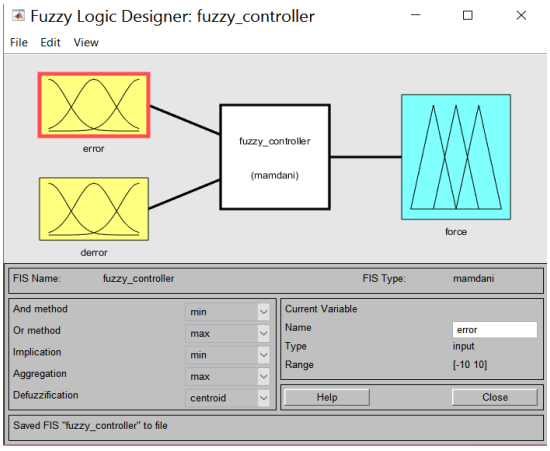

Figure 23: Fuzzy Logic Toolbox Implementation

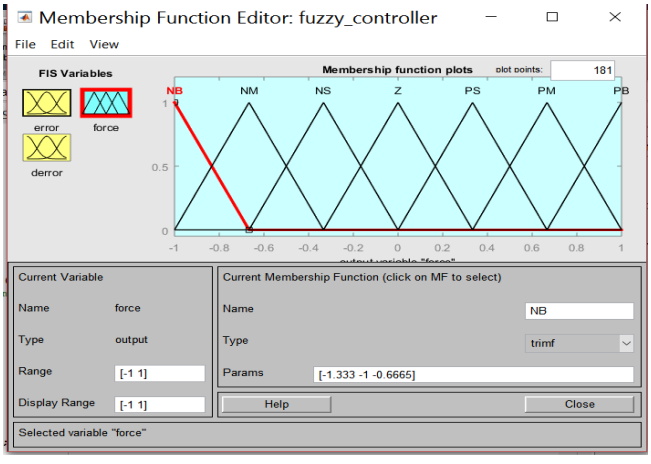

Figure 24: Fuzzy Logic Input Rule Set

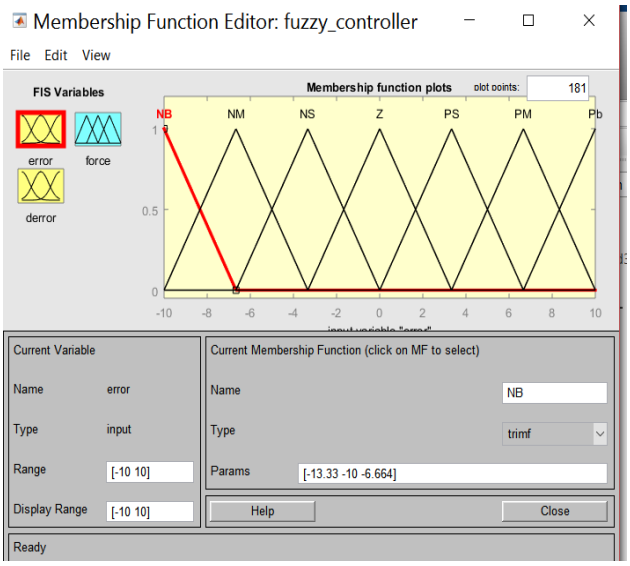

Figure 24: Fuzzy Logic Output Rule set

The K matrix from LQR is the same one as implemented in Section 5.2.3.

$$\boldsymbol{Q} = diag(5, 50, 50, 20, 700, 700)$$
R=1

$$\boldsymbol{K}_{optimal} = [2.23, -403.74, 483.05, 7.99, -14.12, 75.15]$$

This K matrix is used in generating the Information Fusion Function, which is implemented as described in the theory.

In terms of actual implementation, due to the range parameters of the input and output of the Fuzzy Logic system.

There was a necessity to implement gain compensation for Error, ΔError and the output (i.e. Force). The gains were manually tuned to achieve the required controller performance. Table 5 shows the specific tuned gains

Table 5: Fuzzy Logic Tuned gains

Gain	Magnitude
Error Gain	0.1
$\Delta Error$ Gain	0.09
Output Gain	66

- **Simulink Implementation**

The Information Fusion Function implemented in Simulink is shown in Figure 26.

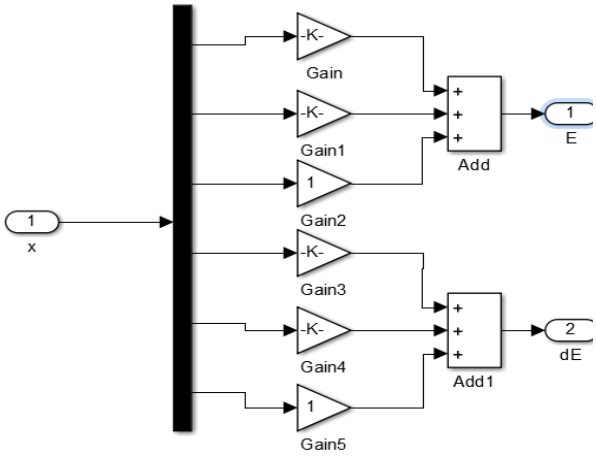

Figure 26: Simulink Information Fusion Function

The overall Fuzzy Logic Control using LQR and Information Fusion is shown in Figure 27.

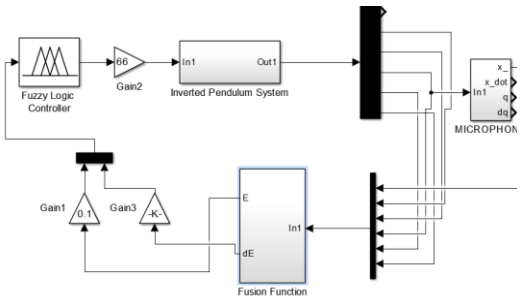

Figure 27: Overall Double Pendulum system with microphone and Fuzzy Logic

5.2.5. Luenberger Full Order State Observer

- *Theory of observer/estimator*

A Luenberger State Observer is incorporated to add real world applicability to the system simulation. The base assumption made in Section 2.3 is that the engineer has access to all state variables, aside from displacement of the cart (which the microphone measures). As a consequence, of the microphone measurement all the states are accessible for state feedback.

However, in reality this is not the case. In real pendulum systems, some of the states are difficult to measure. For example: $\dot{\theta}_1$ and $\dot{\theta}_2$. Hence, an observer or estimator is designed to estimate the difficult to measure states, using some of the other known state variables.

A full order state observer fulfils this role by estimating all the state variables of the system [12]. An estimate of $\boldsymbol{x}$ called $\hat{\boldsymbol{x}}$ is the output from the observer [12].

If an observer is in open-loop the estimated state and actual state will diverge. A Luenberger Observer mitigates this problem by estimating the output vector $\hat{\boldsymbol{y}}$.

The equation of the observer to find $\hat{\boldsymbol{x}}$ in state space notion is given in Equation 119 below:

$$\dot{\hat{x}} = (\mathbf{A} - \boldsymbol{K_e C})\hat{x} + \mathbf{Bu} + \boldsymbol{K_e} y \quad (119)$$

Where $\boldsymbol{K_e}$ is the observers gain matrix (using pole placement).

According, to [12] the choice of these closed loop poles must be 5 times faster than the desired closed loop poles of the system.

Hence, the observers poles should be 5 times to the left (i.e. LHP) in order to be fast enough. Once the observer poles are determined the observer gain matrix (K_e) can be determined via pole placement methodologies such as Direct Comparison in the same way as Section 5.2.2.

- *Controller Implementation*

A full order Luenberger state observer is implemented to estimate unknown states. It is assumed that $x\ (cart\ displacement)$ is measured by the microphone and θ_1, θ_2 and $\dot{x}$ are known. The observer will estimate $\dot{\theta}_1$ and $\dot{\theta}_2$.

The implementation is as per Figure 28 from [12]. The Luenberger Observer is highlighted in red.

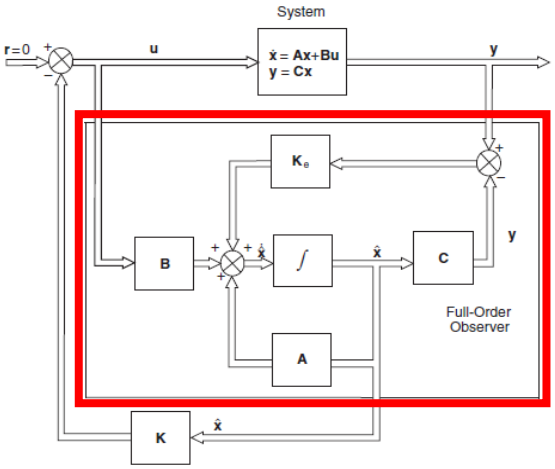

Figure 28: Luenberger Full State Observer (from[12])

s per section 5.2.2, the desired close loop poles for the double pendulum system is:

$\mu 1 = -9.999 + 13.642i$
$\mu 2 = -9.999 - 13.643i$
$\mu 3 = -29.997 + 40.928i$
$\mu 4 = -29.997 - 40.928i$
$\mu 5 = -49.996 + 68.215i$
$\mu 6 = -49.996 - 68.215i$

Thus, based on the theory that the observers closed loop poles must be 5 times faster, the observer poles would simply shift the above poles 5 times to the left hand plane.

After multiplying the system poles by -5 (i.e. shift 5 times into LHP), the observer gain matrix ($\boldsymbol{K_e}$) is determined. The matrix $\boldsymbol{K_e}$ **is as follows:**

$\boldsymbol{K_e} = [$**-1210287, 2654, -70442…**
1354638, 175423, -251806]

- *Simulink Implementation*

The Luenberger sub-system implemented in Simulink is shown in Figure 29.

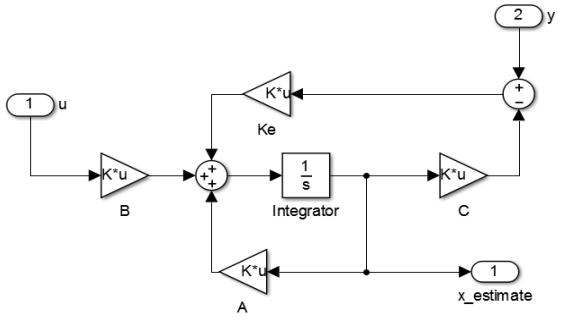

Figure 29: Luenberger Full State Observer

The overall system including the Luenberger observer is shown in Figure 30.

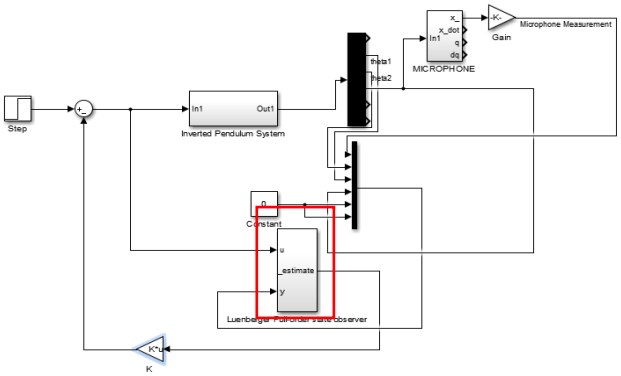

Figure 30: Overall Double Pendulum system with state feedback and a Luenberger Observer.

5.2.6. PID Control

A PID controller for a double pendulum could not be implemented for due to there being an unstable pole in the positive plan going to positive infinity for all values of K. This can be seen in the Root Locus in Figure 6.

A PID would be possible if we change the parameters of the system.

6. RESULTS

Controller simulations for both single and double inverted pendulum systems with each of the designed controllers are carried out in order to compare performance.

6.1. Microphone Measurement System

Firstly, it is important to quantify the performance of the microphone measurement system. The system takes in drag force, by using the velocity of the cart.

The output measurement is the capacitor displacement, which is linearly scaled by a factor of 203 to get cart displacement.

In Figure 31 below, there is a comparison of the measured cart displacement vs the real cart displacement in order to assess accuracy of the measurement.

N.B: ALL OF THE FORTHCOMING CONTROLLER RESULTS TAKE THE MICROPHONE MEASUREMENT AS A STATE INPUT

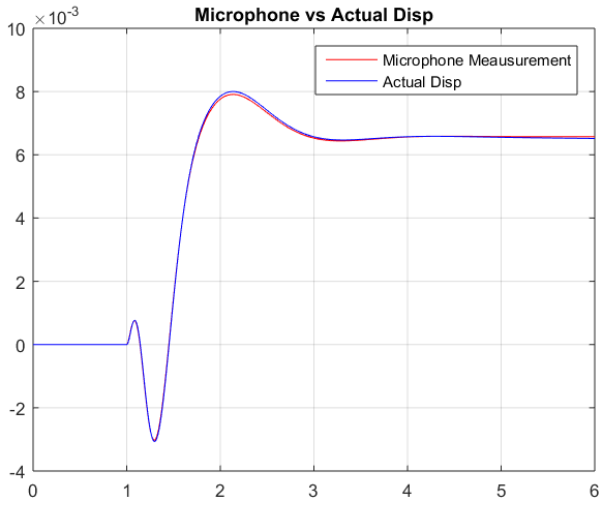

Figure 31: Comparison of the microphone measured displacement of the cart vs the Real displacement of the cart.

6.2. Single Linked Inverted Pendulum

6.2.1. State Feedback (Pole placement)

- Repeated Poles vs Non-repeated Poles

Based on the desired closed loop characteristic equation and by virtue the desired closed loop poles.

A simulation was done comparing the step response for state feedback using pole placement for the repeated and non-repeated poles as discussed in Section 5.1.2

Figure 32 compares the step response of the state feedback system for the repeated poles and non-repeated poles.

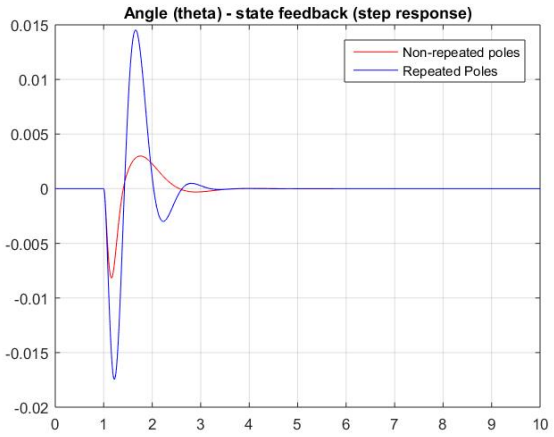

Figure 32: Comparison of the step response for a single pendulum with state feedback. Repeated vs Non-repeated pole placement is compared.

Table 6 below compares the transient behaviour.

Table 6: Transient behaviour of repeated pole vs non-repeated pole state feedback

Parameter	Repeated Poles	Non-repeated Poles
Settling Time (s)	2.4126	2.2298
Overshoot (%)	1.4	0.3

Additionally, the 2 methods of pole placement are compared by initially displacing the angle of the pendulum to 0.1 rad.

The comparative result can be seen in Figure 33

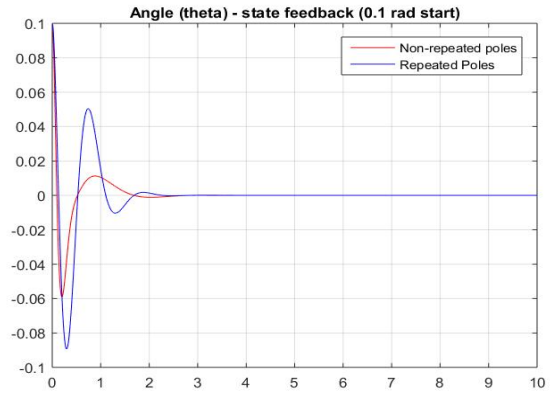

Figure 33: Comparison of the response for a single pendulum with state feedback. Repeated vs Non-repeated pole placement is compared for an initial angle of 0.1 rad.

- Linear System vs Non-Linear System

The controller is designed for the linearized single pendulum system. It would be useful to characterize the controller performance on the non-linear system. Thus, simulations are done comparing the step response for both the linear vs non-linear system.

Figure 34 below shows the step response of the repeated poles (state feedback controller) applied to both the linear and non-linear pendulum systems.

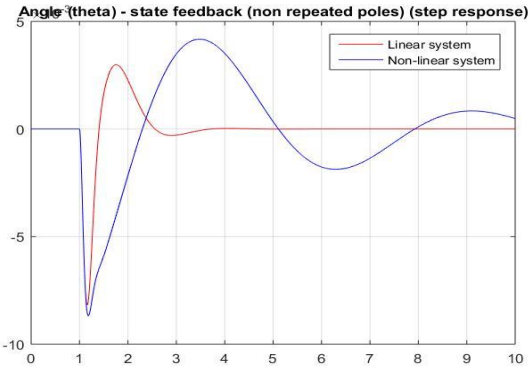

Figure 34: Comparison of the step response the repeated poles state feedback controller applied to the linear system vs non linear system

Table 7 below compares the transient behaviour for both linear and non-linear application

Table 7: Transient behaviour of when applied to the Linear vs Non-Linear system

Parameter	Linear System	Non-Linear System
Settling Time (s)	2.1681	7.4474
Overshoot (%)	0.45	0.55

6.2.2. *Linear Quadratic Regulator (LQR)*

LQR hinges on the designer choosing appropriate weighting matrices **Q** and **R**, as these values influence the optimal feedback gain matrix.

In Section 5.1.3, four different LQR scenarios were proposed and simulated in order to compare the influence of the Q and R parameters on performance.
Figure 35 below illustrates the comparison of step response between the 4 proposed LQR implementations.

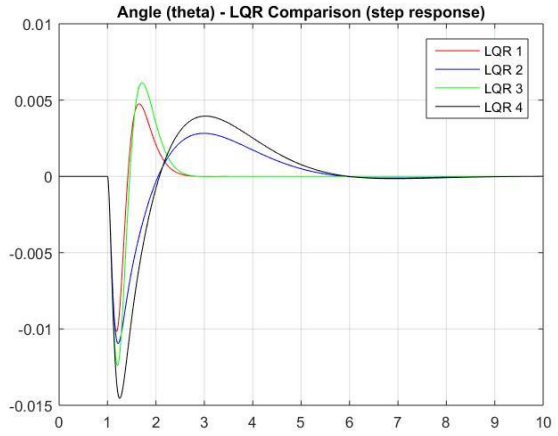

Figure 35: Step Response comparison between 4 different LQR control implementations

6.3. *Double Linked Inverted Pendulum*

6.3.1. *State Feedback (Pole placement)*

Based on the single inverted pendulum displaying superior performance for pole placement with non-repeated roots, it was decided that for the double inverted pendulum that scenario would be simulated.

Section 5.2.2 discusses the pole locations, as well as, the implemented K state feedback gain matrix. The double inverted pendulum system is thus, simulated with that controller in mind.

The step response for the Section 5.2.2. designed controller is illustrated in Figure 36 for θ_1 and Figure 37 for θ_2.

6.3.2. *Linear Quadratic Regulator (LQR)*

The single pendulum simulation of LQR served to demonstrate relationships about the magnitude of the Q and R matrix in system performance.

The simulation of LQR for a double pendulum compares performance when penalizing the error terms $(x\ ,\theta_1\ ,\ \theta_2)$
for not being zero vs penalizing the rate of change of error terms $(\dot{x}\ \ \dot{\theta}_1\ \ \dot{\theta}_2.)$ not being zero.

The Q and R matrices are defined in Section 5.2.3.

Figure 36 for θ_1 and Figure 37 for θ_2 illustrates the step response for two controllers: LQR 1 and LQR 2. Where LQR 1 penalizes $(x\ ,\theta_1\ ,\ \theta_2)$ and LQR 2 penalizes $(\dot{x}\ \dot{\theta}_1\ \ \dot{\theta}_2.)$.

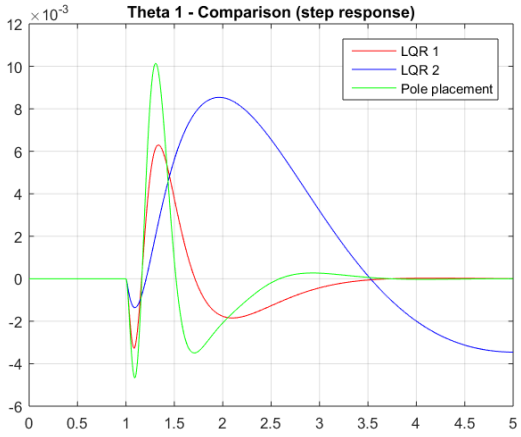

Figure 36: Comparative Step Response for θ_1 for different controller implementations

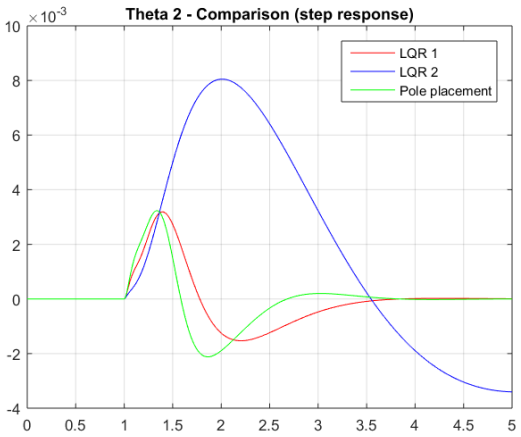

Figure 36: Comparative Step Response for θ_1 for different controller implementations

6.3.3. Fuzzy Logic Control (Intelligent control)

The implementation of the Fuzzy Logic Controller is outlined in Section 5.2.4. The simulations are based on those parameters outlined. Figure 37 represents the response for θ_1 and θ_2 for an initial angle of 0.1 rad.

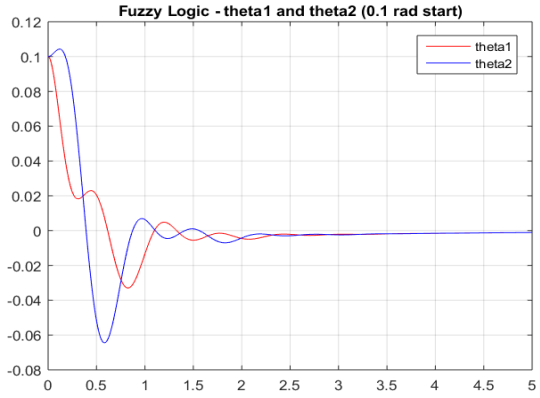

Figure 37: Fuzzy Logic Control for θ_1 and θ_2 for an initial angle of 0.1 rad.

A comparison of Fuzzy Logic and other controllers is in Section 7 (Critical Analysis).

6.3.4. Luenberger Full Order State Observer

The Luenberger Full Order State Observer is firstly tested alone (without the microphone system) in order to prove functionality of the observer. Furthermore, the independent initial test is to assess accuracy of the implemented observer.

Thereafter, the microphone circuit is linked back to the circuit and the observer is tested again.

For both simulations the parameters are as documented in Section 5.2.5.

- Luenberger Observer Alone

Figure 38 illustrates the comparison of real cart displacement (top axis) and Luenberger estimated cart displacement (bottom axis).

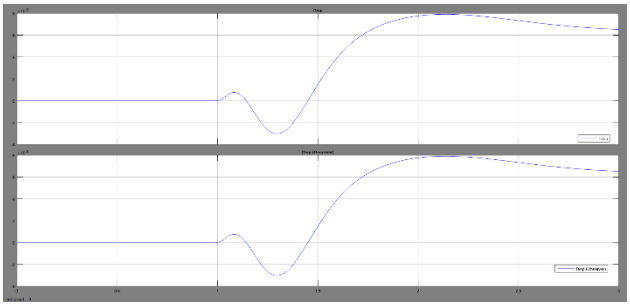

Figure 38: Comparison of real cart displacement (top axis) and Luenberger estimated cart displacement (bottom axis).

Figure 39 illustrates the comparison of real θ_1 (top axis) and Luenberger estimated θ_1 (bottom axis).

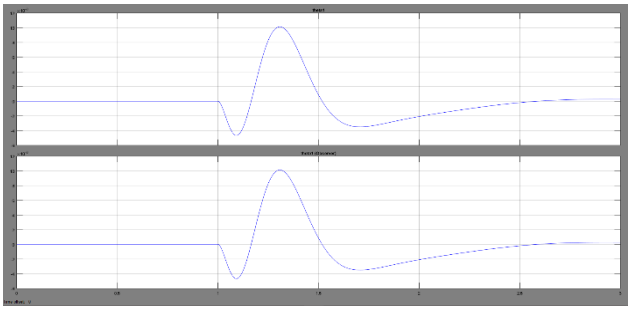

Figure 39: Comparison of real θ_1 (top axis) and Luenberger estimated θ_1 (bottom axis).

Figure 40 illustrates the comparison of real θ_2 (top axis) and Luenberger estimated θ_2 (bottom axis).

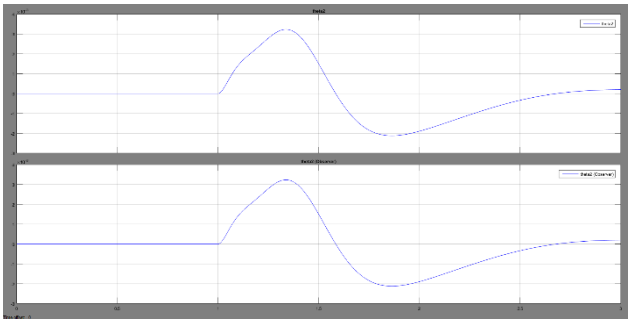

Figure 40: Comparison of real θ_2 (top axis) and Luenberger estimated θ_2 (bottom axis).

- Observer with microphone

After proving the functionality of the Luenberger Observer, the microphone system is incorporated and simulations run as per the Section 6.3.4.

Figure 41 illustrates the comparison of real cart displacement (top axis) and Luenberger estimated cart displacement (bottom axis).

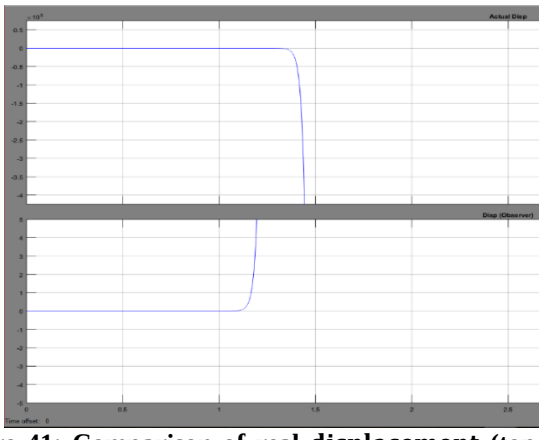

Figure 41: Comparison of real displacement (top axis) and Luenberger estimated displacement (bottom axis) WITH microphone as an input.

Figure 42 illustrates the comparison of real θ_1 (top axis) and Luenberger estimated θ_1 (bottom axis).

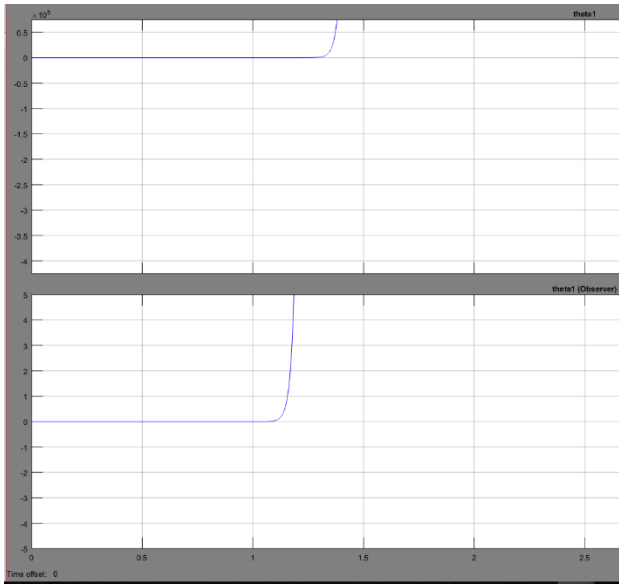

Figure 42: Comparison of comparison of real θ_1 (top axis) and Luenberger estimated θ_1 (bottom axis) WITH microphone as an input.

Figure 43 illustrates the comparison of real θ_2 (top axis) and Luenberger estimated θ_2 (bottom axis).

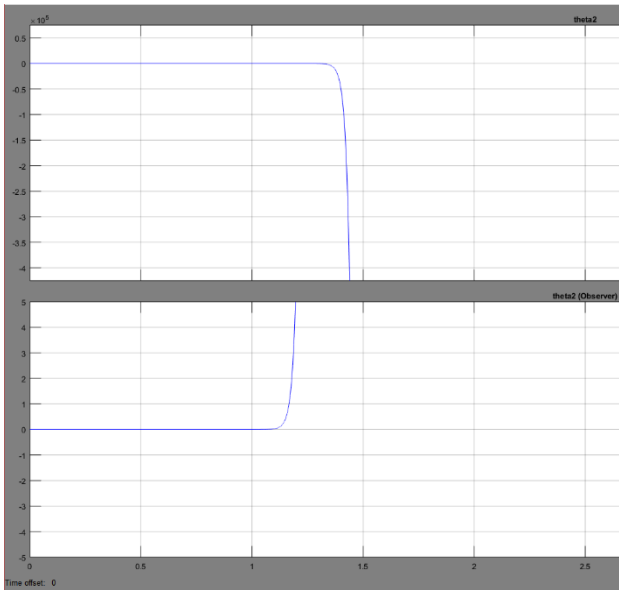

Figure 43: Comparison of comparison of real θ_2 (top axis) and Luenberger estimated θ_2 (bottom axis) WITH microphone as an input.

7. CRITICAL ANALYSIS

7.1. Microphone

It can clearly be seen in Figure 31 that the microphone was successful in measurement of cart displacement. When plotting the measured displacement (after scaling) to the real cart displacement, it can be seen in Figure 31 that the lines overlap with minimal error, implying accurate measurement.

The measurement error is quantitatively seen in Figure 44 and the error of measurement is of order (10^{-4}) which implies accurate measurement.

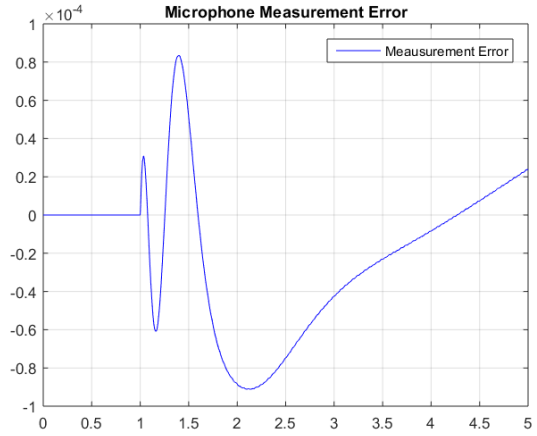

Figure 44: Microphone Measurement Error

7.2. Single Linked Inverted Pendulum

- Successes

It can clearly be seen that both methods of state feedback control using pole placement and LQR were successful in controlling the under actuated and unstable system. Both control systems met the design specifications of 2 second settling time and 10% overshoot. This is illustrated in both Table 8 and Figure 45.

Table 8: Response comparison for a single pendulum between pole placement and LQR

Parameter	Pole Placement	LQR
Settling Time (s)	2.2987	.1681
Overshoot (%)	0.3	0.45

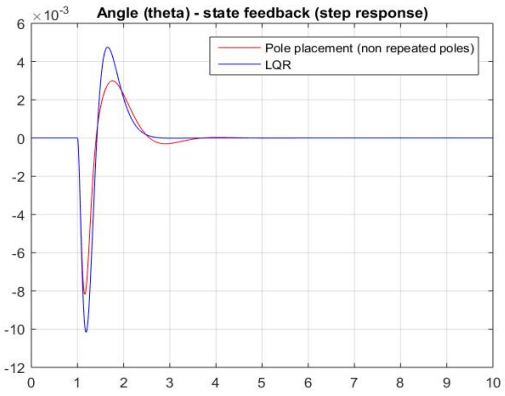

Figure 45: Step Response comparison for a single pendulum between pole placement and LQR

When analysing Table 8 and Figure 45 that between pole placement and LQR there is a trade-off:

- LQR: has faster settling time
- Pole placement: has a smaller overshoot

Thus, as an engineer when deciding between the two, there is clearly a trade-off between settling time and overshoot.

Moreover, it was found that based on the results from Table 6 and Figure 32, that pole placement with non-repeated poles (dominant poles and then further left poles) had the best performance (faster settling time and smaller overshoot). This is opposed to repeated pole placement of the dominant poles. The reason is that by pushing the 2nd set of poles further left of the dominant poles it reduces the influence, rather than overshadowing the dominant poles.

Lastly, with regard to LQR, Figure 35 highlights the relationship of the Q and R matrix to the transient behaviour. Clearly, the R matrix (cost of control) does not play as big a role. The Q matrix has a bigger influence. The relationship is the larger the values in the Q matrix, the faster the transient behaviour.

- Failures

The state feedback controller was tested on both the linear and non-linear pendulum systems. The controller performed to designed specifications for the linear system. However, the controller failed to meet specifications when tested against the non-linear system. The non-linear system is controlled and stabilized, just not to the design specifications. As Table 7 documents for example the settling time is 7.44 seconds rather than 2 seconds.

The reason for this is that the controller is designed for the linear pendulum model (which is simplified) and thus, not the same behaviour as the real non-linear system. The linearized system is an approximation of the real system due to small angle approximations, as well as, linearization around 0 (equilibrium).

Hence, because the controller is designed with reference to the simplified model, it does not factor in all the system complexities. Therefore, it explains why the performance specifications are unable to be met.

7.3. Double Linked Inverted Pendulum

- Successes

The 3 controllers (state feedback, LQR, Fuzzy Logic) investigated for the double inverted pendulum were all successful in achieving the design specifications.

Figure 46 shows the comparison of all implemented controllers for θ_1 and Figure 47 for θ_2 for a start angle of 0.1 rad

Figures 48 shows the comparison of of all implemented controllers for θ_1 And Figure 49 for θ_2 for a start angle of 1.57 rad (90 degrees).

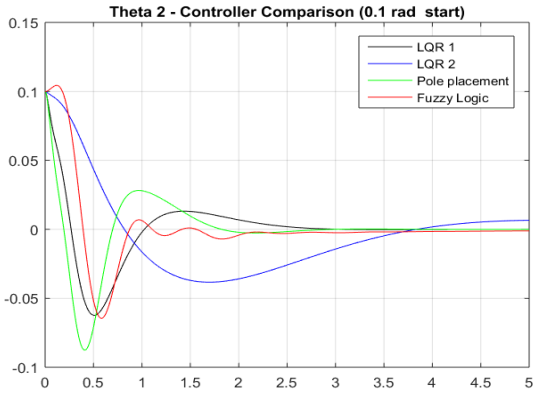

Figure 46: Controller comparison for θ_1 for a start angle of 0.1 rad

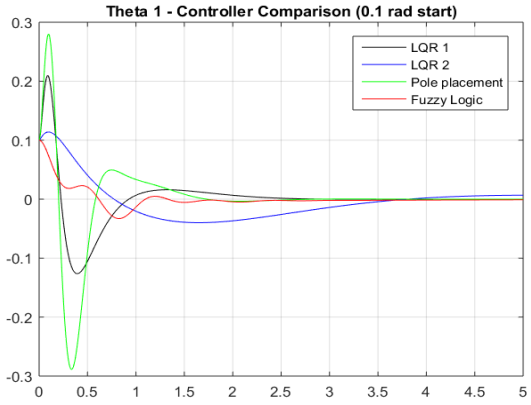

Figure 47: Controller comparison for θ_2 for a start angle of 0.1 rad

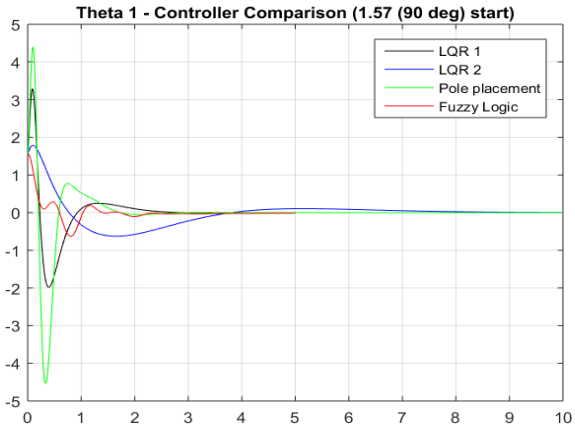

Figure 48: Controller comparison for θ_1 for a start angle of 1.57 rad

Figure 49: Controller comparison for θ_2 for a start angle of 1.57 rad

It can be seen from the Figures 46-49 , that in fact the Fuzzy Logic controller had the most superior performance of all the 3 controllers. That being said, Pole placement and LQR still had performance, which met the design specifications, which make them successful.

However, as an engineer based on the results, the Fuzzy Logic controller would be the best control option. The reason is not only can it meet the design and performance specifications, but Fuzzy Logic has the advantage over the other 2 controllers, as it does not require design based on a system mathematical model. So, if an additional link is added to the pendulum (to make it 3), then Fuzzy Logic would not require additional mathematical modelling of a more complex system.

Moreover, the usage of the Information Fusion Function reduced the number of rules – therefore making Fuzzy Logic more applicable, as well as, less computationally expensive.
Thus as a rule based on analysis of both single and double pendulum control - could be said that state feedback (pole placement and LQR) methods are simpler on less complicated systems such as a single inverted pendulum. Hence, is most applicable for simpler and lower order systems where the modelling is easy.

However, Fuzzy Logic has the advantage when applied to more complex systems (such as the double inverted pendulum). The reason being is that Fuzzy Logic control does not require a mathematical model, whilst still adequately performing.

- Failures

The Luenberger observer performed well when the microphone was excluded. Figures 38-40, show that the estimated states clearly match the real states.

However, when the microphone is added (which measures cart displacement), then the observer no longer works as expected (as can be seen in Figures 41-43).

The reason for the state observer to fail when the microphone is included is due to the measurement error that can be seen in Figure 44.

More importantly, the assumption relating plate displacement and cart displacement, was that there is a linear relationship. For that reason, a linear gain was applied on plate displacement to get to cart displacement.

However, as can be seen in Figure 50, the actual relating scaling factor between the two is NON-LINEAR. Especially, at the beginning there are non-linear spikes (highlighted in red) before the linear relationship (highlighted in green) takes over. Thus, the non-linearity circled in red would account for the failure of state estimation when the microphone is included due to the error introduced.

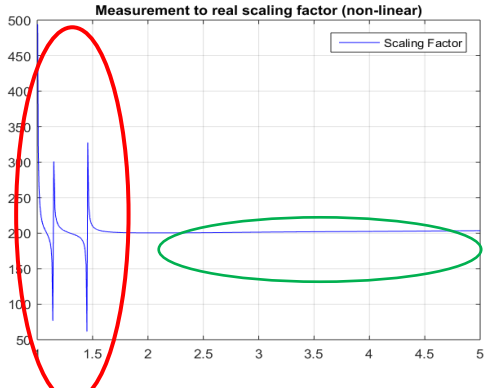

Figure 50: Non-linear scaling factor between microphone x and real

8. FUTURE RECOMMENDATIONS

The most important future recommendation will be to implement a non-linear controller on the system as currently, the controllers implemented in this paper only work for the linear system, making the designs not effective in a real-world application. For example: 2 methods which could be explored are: (1) Sliding Mode Control and (2) Non-linear artificial neural network control.

More sensors can be used to measure multiple states as measuring a single state is prone to error, meaning that if the sensor has some measurement error in it this would affect the estimator and therefore the entire system. Multiple sensors also add to system robustness that if one sensor is fails, the other measurements won't be affected by it.

A Kalman Filter can be explored as an alternative estimator to the Luenberger Observer – especially due to the Kalman Filters ability to noise tolerance in the measurement. Thus, potentially it would function well even with measurement errors. The Kalman filter can then be linked with an LQR K matrix – to form an LQG controller.

9. CONCLUSION

In conclusion, both single and double linked pendulum systems have been successfully modelled using both Force and Lagrange analysis. Additionally, a microphone was implemented and successfully measured cart displacement with an error of magnitude (10^{-4}). Controllers were implemented for both single and double inverted pendulum systems, with a Luenberger observer also implemented for the double pendulum system. The controller topologies that were explored was state feedback via pole placement, optimal control using LQR based state feedback, classic control using PID and intelligent control through Fuzzy Logic. All of the controllers, beside PID which could not be implemented, performed to meet the design criteria of 2s settling time and 10% overshoot. It can be said that state feedback methodologies are simpler and better applied to simpler systems, whilst Fuzzy Logic should rather be chosen on systems with increasing degrees of complexity.

REFERENCES

[1]H. Niemann and J. Poulsen, "Design and analysis of controllers for a double inverted pendulum", *ISA Transactions*, vol. 44, no. 1, pp. 145-163, 2005.

[2]"Mathematical model of a pendulum on a cart", *Finn Haugen*, 2017. [Online]. Available: http://techteach.no/simview/pendulum/pendulum_model.pdf. [Accessed: 23- Mar- 2017].

[3]F. jeremic, "Derivation of Equations of Motion for Inverted Pendulum Problem", 2017. [Online]. Available: http://www.cas.mcmaster.ca/~qiao/courses/cs4xo3/presentations/InvPend.pdf. [Accessed: 23- Mar- 2017].

[4]J. Stellet, "Control of an Inverted Pendulum", 2017. [Online]. Available: http://jstc.de/blog/uploads/Control-of-an-Inverted-Pendulum.pdf[Accessed: 23- Mar- 2017].

[5]M. Grossman, "N-link inverted pendulum, LQR control, some observations", 2017. [Online]. Available: http://www.atpjournal.sk/buxus/docs/casopisy/atp_plus/plus_2008_1/plus62_65.pdf. [Accessed: 26- Mar- 2017].

[6]"Stabilization of Rotary Inverted Pendulum Using Fuzzy Logic", *International Journal of Intelligent Information Processing*, vol. 2, no. 4, pp. 23-31, 2011.

[7]A. Jose, C. Augustine, S. Malola and K. Chacko, "Performance Study of PID Controller and LQR Technique for Inverted Pendulum", *World Journal of Engineering and Technology*, vol. 03, no. 02, pp. 76-81, 2015.

[8]"Stabilization of Rotary Inverted Pendulum Using Fuzzy Logic", *International Journal of Intelligent Information Processing*, vol. 2, no. 4, pp. 23-31, 2011.

[9]M. Shehu, "LQR, double-PID and pole placement stabilization and tracking control of single link inverted pendulum", 2017.

[10]M. Roon, "Design and Control of an Inverted Pendulum", 2017. [Online]. Available: http://homepages.wmich.edu/~kamman/IP_FINAL_PROJECT_REPORT.pdf. [Accessed: 25- Mar- 2017].

[11]"Control Tutorials for MATLAB and Simulink - Inverted Pendulum: State-Space Methods for Controller Design", *Ctms.engin.umich.edu*, 2017. [Online]. Available: http://ctms.engin.umich.edu/CTMS/index.php?example=InvertedPendulum&section=ControlStateSpace. [Accessed: 22- Mar- 2017]

[12]R. Burns, *Advanced control engineering*, 1st ed. Oxford: Butterworth-Heinemann, 2001.

[13]A. Kumar, S. Kundu and V. Kumar, "Evolving Single Input FLC for Double Inverted Pendulum", *ICSCTI*, no. 978, pp. 34-38, 2015.

[14] L. Wang, S. Zheng, X. Wang and L. Fan, "Fuzzy Control of a Double Inverted Pendulum based on Information Fusion", *IEEE*, no. 978, pp. 327-330, 2010